Supporting Information

Mutasynthesis Generates Nine New Pyrroindomycins

Zhuhua Wu,[a,b,†] Zhenxiang Xia,[b, c,†] ZhiJun Tang, [b,*] Ji'an Li,[a,*] Wen Liu [b,*]

[a] National key Laboratory of Lead druggability Research, Shanghai Institute of Pharmaceutical Industry, China State Institute of Pharmaceutical Industry, 285 Copernicus Road, Shanghai 201203, China.

[b] State Key Laboratory of Chemical Biology, Shanghai Institute of Organic Chemistry, University of Chinese Academy of Sciences, Chinese Academy of Sciences, 345 Lingling Road, Shanghai 200032, China.

[c] Department of Pharmacy, Stomatological Hospital and Dental School of Tongji University, Shanghai Engineering Research Center of Tooth Restoration and Regeneration, 399 Middle Yan Chang Road, Shanghai, 200072, China.

[*] To whom correspondence should be addressed: Shanghai Institute of Organic Chemistry, Chinese Academy of Sciences, 345 Lingling Rd., Shanghai 200032, China. Zhijun Tang, Email: tangzj@sioc.ac.cn; Ji'an Li, E-mail: liji_an@hotmail.com; and Wen Liu, Email: wliu@sioc.ac.cn, Tel: 86-21-54925111, Fax: 86-21-64166128

[†] These authors equally contributed to this work.

Table of Contents

1. Experimental Procedures

1.1 General Experimental Procedures.

Materials, Strains, Plasmids and Primers. Biochemicals and media were purchased from Sinopharm Chemical Reagent Co., Ltd. (China), Oxoid Ltd. (U.K.) or Sigma-Aldrich Co. LLC. (USA) unless otherwise stated. Restriction endonucleases were purchased from Thermo Fisher Scientific Co. Ltd. (USA). Chemical reagents were purchased from standard commercial sources. The bacterial strains, plasmids and primers used in this study are summarized in Tables S1 and S2, respectively.

DNA isolation, Manipulation and Sequencing. DNA isolation and manipulation in *Escherichia coli* and *Streptomyces rugosporus* were carried out according to standard methods.1-4 Amplifications by polymerase chain reaction (PCR) were carried out on an Applied Biosystems Veriti Thermal Cycler (Thermo Fisher Scientific Inc., USA) using either Taq DNA polymerase (Vazyme Biotech Co. Ltd., China) for routine verification or PrimeSTAR HS DNA polymerase (Takara Biotechnology Co., Ltd., Japan) for high fidelity amplification. Primer synthesis was performed at Shanghai BioSune Biotech Co. Ltd. (China). DNA sequencing was performed at Shanghai TSINGKE Biotech Co. Ltd. (China).

Sequence Analysis. Open reading frames (ORFs) were identified using the FramePlot 4.0 beta program (http://nocardia.nih.go.jp/fp4/). The deduced proteins were compared with other known proteins in the databases using available BLAST methods (http://blast.ncbi.nlm.nih.gov/Blast.cgi). Structure modles were built using AlphaFold2.0 and displayed via Pymol.

Chemical Analysis. High performance liquid chromatography (HPLC) analysis was carried out on an Agilent 1260 HPLC system (Agilent Technologies Inc., USA) equipped with a DAD detector. Semi-preparative HPLC was performed on an Agilent 1100 system. HPLC-electrospray ionization-mass spectrometry (HPLC-ESI-MS) and ESI-MS/MS were performed on a Thermo Fisher LTQ Fleet ESI-MS spectrometer (Thermo Fisher Scientific Inc., USA), and the data were analyzed using Thermo Xcalibur software. ESI-high resolution MS (ESI-HR-MS) analysis was carried out on an instrument consisting of a 1260 HPLC system and a 6538 UHD quadrupole time of flight (QTOF) high resolution mass spectrometry (Agilent Technologies, Santa Clara, USA). NMR data were recorded on a Bruker AV-500 (Bruker Co. Ltd, Germany).

1.2 Construction of the *pyrK1* Gene Inactivation Strain.

To inactivate *pyrK1* by in-frame deletion, the 2.370 kb fragment obtained by PCR using the primers K1-L-for/rev and the 2.252 kb fragment obtained by PCR using the primers K1-R-for/rev were cloned into the *Eco*RI-*Hind*III site of pKC1139, resulting in the generation of the recombinant plasmid pWL1001. It should be noted that within this plasmid, a specific 600 bp coding region of *pyrK1* was deleted. To transfer pWL1001 into *Streptomyces rugosporus* NRRL 21084, conjugation between *S. rugosporus* and *E. coli* ET12567 harboring pWL1001 was performed according a

method described previously,[3] yielding the recombinant strain WL1001. Breifly, approximately 10^9 *S. rugosporus* spores were suspended in TES (500 mL, 0.05 M, pH 8.0) and shocked by heating at 50℃ for 10 min. TSB (500 mL) was then added for further incubation at 37℃ for 3–5 h. Spores were recovered by centrifugation and resuspended in LB medium (2 mL) for recipient preparation. *E. coli* ET12567containing the pWL1001 plasmid was grown in LB medium with apramycin to an OD_{600} of 0.4–0.6. Cells from 50 mL of culture were recovered by centrifugation, washed twice with 20 mL LB medium, and resuspended in LB medium (1 mL) for use as the donor. Donor (100 mL) and recipients (100 mL) were mixed and distributed onto MS plates supplemented with 10 mM $MgCl_2$. The plates were incubated at 30℃ for 10–16 h and then overlaid with 1 mL water of containing nalidixic acid and apramycin (50 mg/mL) for *S. rugosporus* exconjugant selection. Incubation was continued at 30℃ until exconjugants appeared. The colonies demonstrating resistance to apramycin at a temperature of 37℃ were regarded as the integrating mutants, indicating that a single-crossover homologous recombination event had occurred. These mutants were subsequently cultivated on MS agar plates for five rounds in the absence of apramycin. The genotypes of resulting the strains that were apramycin-sensitive were selected and examined by PCR amplification and sequencing, ultimately leading to the identification of the recombinant strain WL1001 in which *pyrK1* was inactivated as designed.

Table S1. Strains and plasmids used in this study

Strain/Plasmid	Relevant Characteristics	Source/Reference
E.coli		
DH5α	Host for general cloing	Invitrogen
ET12567	Donor strain for conjugation between *E.coli* and *Streptomyces*	[1]
Streptomyces rugosporus		
NRRL 21084	Wild type, PYRs producing strain	NRRL
WL1001	*pyr*K1 in-frame deletion mutant, PYR non-producing	this study
Plasmids		
pKC1139	*E.coli-Streptomyces* shuttle vector for gene inactivation, temperature sensitive replication in Streptomyces with apamycin resistance	[2]
pWL1001	pKC1139 derivative containing 2.370 kb and 2.252 kb fragment for in-frame deletion of pyrK1	this study

Table S2. Primers used in this study.

Gene ID	Prmer name	Primer sequence	Relevant characteristics
	K1-L-for	GGGCTGCAGGTCGACTCTAGACATCATCATCAACAACTGCTC	mutant
	K1-L-rev	CGTAGGCGTCGAGCAGCATGCCGAGGTC	construction
	K1-R-for	TGCTGCTCGACGCCTACGAGCGGAACG	mutant
	K1-R-rev	ATCGCGCGCGGCCGCGGATCCTGGTCGGCAGCATCACGC	construction
pyrk1	K1-for	AGATATACATATGCCCCAGACCACGACCCT	mutant
	K1-rev	GTGCTCGAGCCGCCCTTCCGCCGCCCGGC	verification

Figure S1. In-frame deletion of pyrK1 and PCR verification of the mutant strain.

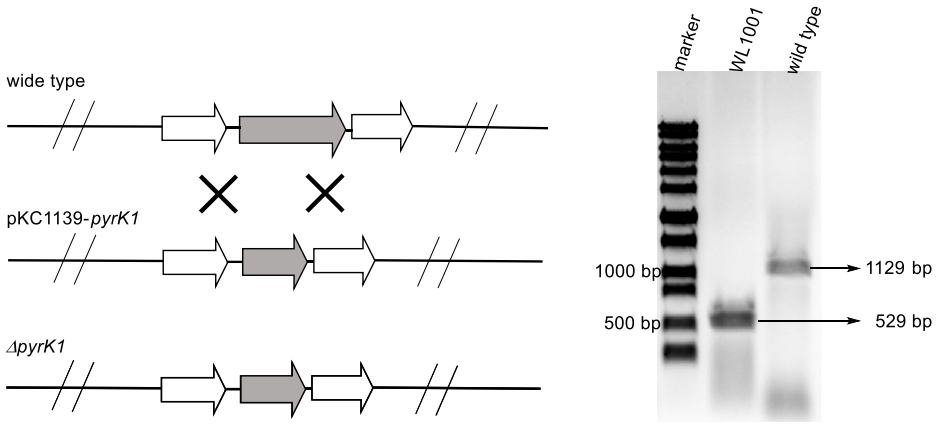

1.3 Fermentation, Chemical Feeding and Metabolic Anaslysis.

The fermentation was conducted following the method previously described by Qiongqiong Wu et al.[1] Breifly, in the primary fermentation, a 5-day cultured seed obtained from MS agar was inoculated into a 250-mL Erlenmeyer flask containing 50 mL of seed medium (composed of glucose 1%, soluble starch 2%, yeast extract 1%, N-Z Amine A 1%, and $CaCO_3$ 0.1% in tap water, pH 7.2). The flask was then incubated at 28°C and 220 rpm for 2 days. For the secondary fermentation, 5 mL of the seed culture broth was transferred into a 500-mL Erlenmeyer flask containing 100 mL of fermentation medium (comprised of glucose 3%, peptone 1%, yeast extract 1%, ammonium ferric citrate 0.1%, and $CaCO_3$ 0.1% in tap water, pH 6.5). This flask was incubated at 28°C and 220 rpm for 7 days. Ethyl acetate (50 mL) and fermentation broth (50 mL) were stirred rigorously under sonication for 20 min followed by centrifugation. The upper organic phase was removed. The solvent was concentrated under reduced pressure, and the residue was dissolved in methanol (1 mL). Product analysis was carried out on an Agilent Zorbax column (SB-C18, 5 μm, 4.6 x 250 mm, Agilent Technologies Inc., USA) using a DAD detector, by gradient elution of solvent A (H_2O containing 0.1 % formic acid) and solvent B (CH_3CN containing 0.1 % formic acid) at a flow rate of 1 mL/min over a 30-min gradient program as fllows: T = 0 min, 30 % B; T = 5 min, 30 % B; T = 20 min, 80 % B; T = 23 min, 80 % B; T = 27 min, 30 % B, and T = 30 min, 30 % B (λ = 315 nm).

In the feeding experiment, aromatic carboxylic acid substrates with a final concentration of 2.5 mM were added during the middle of the logarithmic growth phase in the secondary fermentation. The culture was harvested on the seventh day. Products analysis were performed according to the method decribed above.

1.4 Isolation and Structure Characterization of the Compounds 4 and 5.

A volume of 100 L of fermentation broth from WL1001 was subjected to compounds isolation. The culture medium was centrifuged, and the resulting supernatant was extracted three times with 300 L of ethyl acetate (EtOAc). Following the concentration step, the crude extract was subjected to elution on an MCI CHP20P gel column (Mitsubishi Chemical Corporation, Japan) utilizing methanol solutions with varying concentrations (i.e., 50%, 60%, 70%, 80%, 90%, and 100%, respectively). The fractions corresponding to **4** and **5** were individually collected and subsequently applied onto a Sephadex LH-20 column (Mitsubishi Chemical Corporation, Japan) for further separation. Elution was carried out using methanol as the eluent. After crude concentration, the semipreparation of compound **4**, and **5** by HPLC was conducted on an Agilent Zorbax column (Agilent Zorbax SB-C18, 5 μm, 4.6 mm × 250 mm, Agilent Technologies Inc., USA) by gradient elution (315 nm over a 30-min gradient program: T = 0 min, 30 % B; T = 5 min, 30 % B; T = 20 min, 80 % B; T = 23 min, 80 % B; T = 27 min, 30 % B, and T = 30 min, 30 % B (solvent A, H_2O containing 0.1 % formic acid; solvent B, CH_3CN containing 0.1 % formic acid.)), yielding 16 mg of **4**, and 26 mg of **5** for NMR analysis.

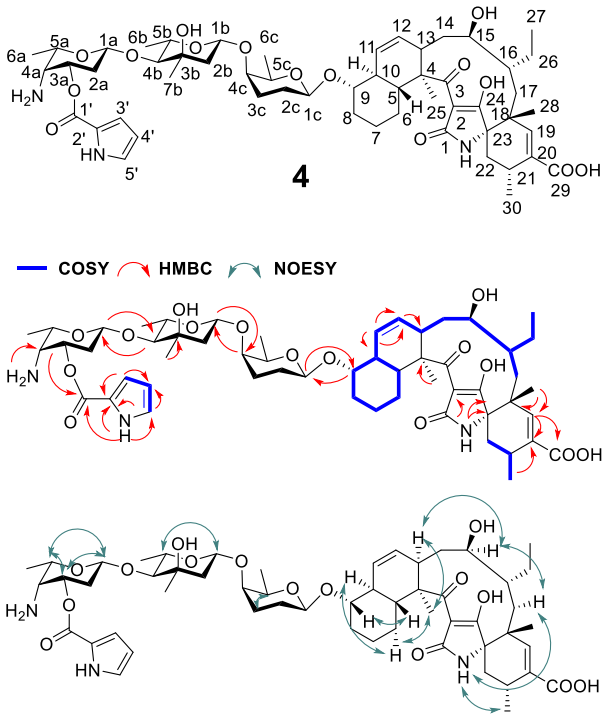

Compound **4** was obtained as colourless gum. HR-ESI-MS analysis of **4** exhibited a $[M+H]^+$ ion at *m/z* 1008.5441, consistent with the molecular formula $C_{54}H_{78}N_3O_{15}$. Investigation of the ^1H and ^{13}C NMR spectra indicated that a pyridine formic acyl group was observed in ^1H NMR (δ_H 11.60, s; 6.90, s; 6.79, s; and 6.11, s) and ^{13}C (δ_C 161.3, 126.2, 121.3, 108.5, and 110.9), one amino proton signal at δ_H 8.14 (1H, brs), one tri-substituted olenic proton signal at δ_H 6.32 (1H, s), two mono-substituted olenic proton signals at δ_H 5.56 (1H, d, J = 14.8, 7.8 Hz), 5.67 (1H, J = 14.8, 10.8 Hz), three anomeric proton in sugar moiety signals at δ_H 4.51 (1H, d, J = 8.5 Hz), 4.73 (1H, brs), and 4.73 (1H, brs), three singlet methyls at δ_H 1.12, 1.26, and 1.76 (3H each, s). Then through analyzing the ^{13}C NMR data, which indicated the existence of one carbonyl carbons at δ_C 201.3, one ester carbon at δ_C 161.3, one amide carbon at δ_C 163.0, one carboxylic acid at δ_C 167.9, six unsaturated carbons at δ_C 198.6, 146.4, 132.0, 132.0, 121.3, and 106.0, three anomeric carbon signals of sugar moiety at δ_C 101.0, 100.1, and 98.6, and 11 oxygenated/ominated carbons at δ_C 84.5, 81.7, 80.6, 75.2, 69.7, 69.7, 68.9, 66.6, 65.8, 63.1, and 51.3. The above data of ^1H and ^{13}C NMR were compared with those of PYR A and B showed they were identical, specifically, except for the data mentioned above of the pyridine formic acyl group. In other hand, given the bioinformatics analysis of the mutant strain product, which also involved in the biosynthesis of the DHPI moiety in PYR. The ^1H–^1H COSY experiment enabled the identification of the pyridine formic acyl group. As shown abbove, the ^1H-^1H COSY spectrum exhibited that H-4' correlated with H-3', H-5' correlated with H-3'. Together with HMBC and HSQC, suggesting a pyridine formic acid formed an ester bond with the hydroxyl at 3a.

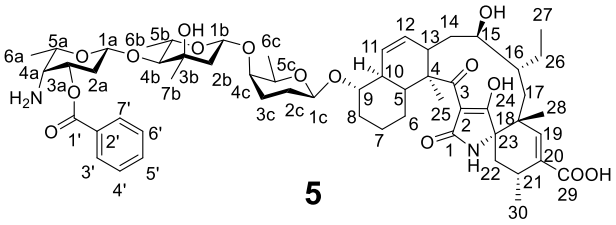

5

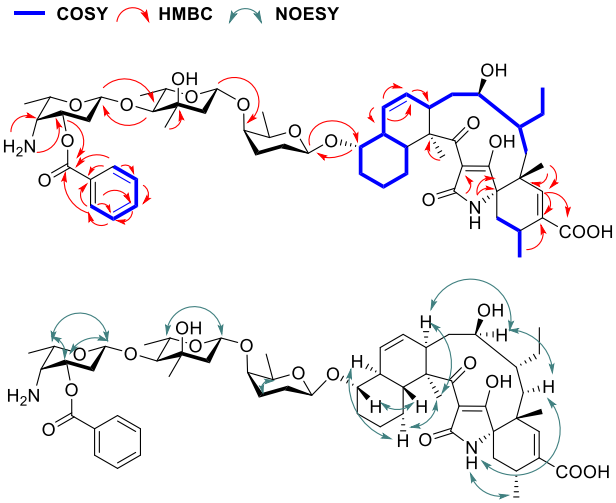

Compound **5** was isolated as colourless gum, whose molecular formula $C_{56}H_{78}N_2O_{15}$ was deduced by HR-ESI-MS ([M+H]$^+$ at *m*/*z* 1019.5488, calcd. 1019.5480). Based on the analysis of the ^{1}H NMR spectrum (Table S3), which suggested the presence of ABX system resonances at δ_H 7.81 (2H, d, *J* = 7.0 Hz), 7.49 (1H, t, *J* = 7.2 Hz) and 7.46 (2H, t, *J* = 7.2 Hz), one amino proton signal at δ_H 8.24 (1H, brs), one tri-substituted olenic proton signal at δ_H 6.29 (1H, s), two mono-substituted olenic proton signals at δ_H 5.46 (1H, brd, *J* = 14.6 Hz), 5.67 (1H, s), three anomeric proton in sugar moiety signals at δ_H 4.70 (1H, *J* = 8.3 Hz), 4.69 (1H, brs), and 4.51 (1H, d, *J* = 9.0 Hz), three singlet methyls at δ_H 1.19, 1.21, and 1.71 (3H each, s). Then through analyzing the ^{13}C NMR data, which indicated the existence of one carbonyl carbons at δ_c 200.8, one ester carbon at δ_c 167.6, one carboxyl carbon at δ_c 168.4, one amide carbon at δ_c 163.8, twelve unsaturated carbons at δ_c 198.7, 148.0, 135.2, 133.2, 131.7, 130.9, 128.2, 128.2, 127.3, 127.3, 120.8, and106.2, three anomeric carbon signals of sugar moiety at δ_c 100.8, 100.1, and 98.5, and and 11 oxygenated/ominated carbons at δ_c 84.3, 82.5, 81.3, 75.2, 69.5, 69.5, 68.9, 65.7, 65.7, 63.1, and 52.1. The above data of ^{1}H and ^{13}C NMR were compared with those of PYR A and B showed they were identical, specifically, except for the data mentioned above of the characteristic ABX system in aromatic ring. However, **5** possessed extremely complex structure with many carbons and protons of similar chemical shifts, and was very difficult to elucidate only according to their NMR data. Comparison of the HR-MS/MS data of PYR-A, PYR-B and **5**, reveled the same pentacyclic aglycone and sugar fragments, but the different acyl fragment, indicating that the aromatic ring in **5** possibly replaced with benzoic acid in pyrroindomycin. To verify this speculation, the following ^{1}H-^{1}H COSY, HMBC, and HSQC experiments were performed. We focused on data of the aromatic ring-substituted deoxytrisaccharide side chain. The ^{1}H–^{1}H COSY correlations, combined with HSQC, DEPT spectra, revealed the existence of the substructures of H-3' to H-4', H-4' to H-5', H-5' to H-6', H-6' to H-7'. In the HMBC spectrum, correlations were observed from H-3' to C-2', C-4', C-7', and C-5', and from H-7' to C-2', C-6', C-

3', and C-5', therefore showing the connection of C-3'–C-2' –C-7'. Other HMBC correlations from H-3' to C-1' and H-7' to C-1' suggested the presence of the benzoyl group. Further HMBC correlation between H-3a and C-1' allowed the link of the benzoyl group to C-3a of deoxytrisaccharide. The inter-sugar linkages were then established on the basis of the HMBC correlations between H-1a (δ_H 4.51) and C-4b (δ_C 84.3), between H-1b (δ_H 4.70) and C-4c (δ_C 75.2), and the sugar-aglycone linkage was determined according to the correlation signal between H-9 (δ_H 3.54) and C-1$_C$ (δ_C 98.5). The relative configuration of dialkyldecalin moiety in **5** was similar to the PYR intermediates in our previous report.

2. Supplementary Results

2.1 HR-MS and HR-MS/MS analysis of 3.

Figure S2. HR-MS ananlyis of 3

Qualitative Analysis Report

Data Filename	915.d	**Sample Name**	
Sample Type	Sample	**Position**	Vial 61
Instrument Name	Instrument 1	**User Name**	
Acq Method	I3.m	**Acquired Time**	9/22/2023 1:35:06 PM
IRM Calibration Status	Success	**DA Method**	FGFUS-C18.m
Comment			

Sample Group **Info.**

Acquisition SW 6200 series TOF/6500 series

Version Q-TOF B.05.01 (B5125.3)

User Spectra

Fragmentor Voltage	Collision Energy	Ionization Mode
75	0	ESI

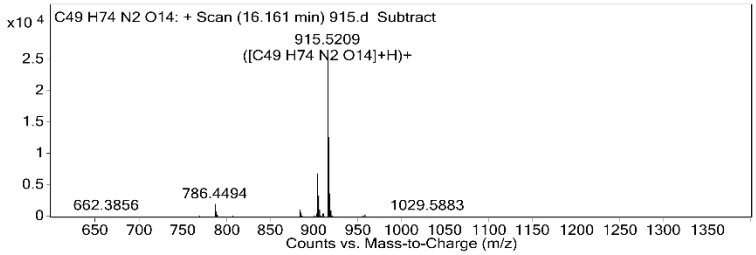

Peak List

m/z	z	Abund	Formula	Ion
915.5209	1	25396.85	C49 H74 N2 O14	(M+H)+
916.5227	1	12772.39	C49 H74 N2 O14	(M+H)+
917.5274	1	3773.54	C49 H74 N2 O14	(M+H)+
918.5256	1	1009.68	C49 H74 N2 O14	(M+H)+
919.5295	1	341.78	C49 H74 N2 O14	(M+H)+

Formula Calculator Element Limits

Element	Min	Max
C	12	70
H	0	120
O	1	20
N	1	4

Formula Calculator Results

Ion Formula	m/z	m/z (Calc)	DBE	Diff (ppm)	Score (MFG)
C64 H69 N O4	915.5209	915.5221	31.5	1.32	98.64
C62 H67 N4 O3	915.5209	915.5208	32	-0.14	99.98
C49 H75 N2 O14	915.5209	915.5213	14	0.42	99.86
C46 H77 N O17	915.5209	915.5186	9.5	-2.51	95.29

--- End Of Report ---

Figure S3. HR-MS/MS comparison of PYR-A (A), PYR-B (B) and 3 (C).

(**A**)

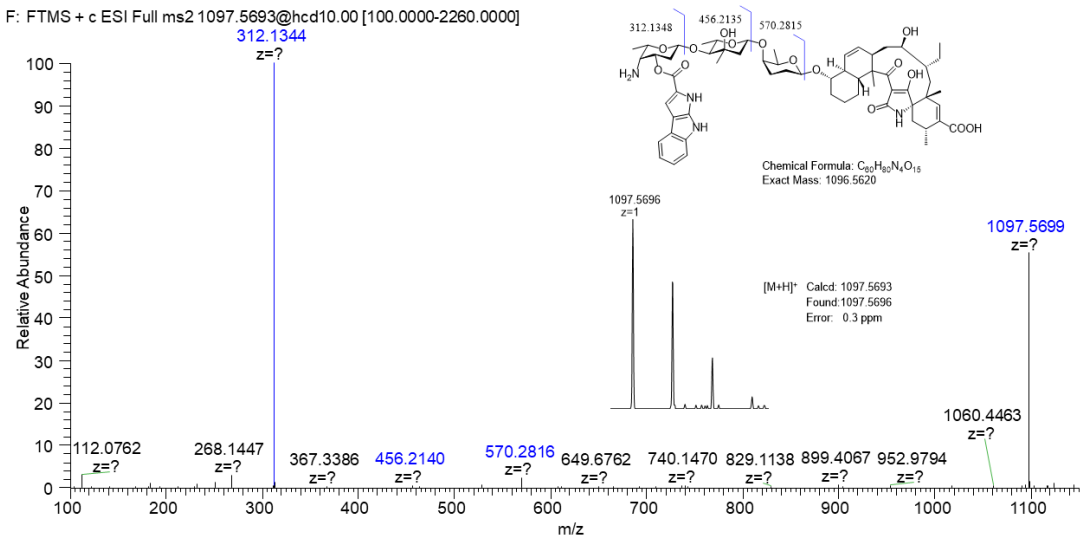

(**B**)

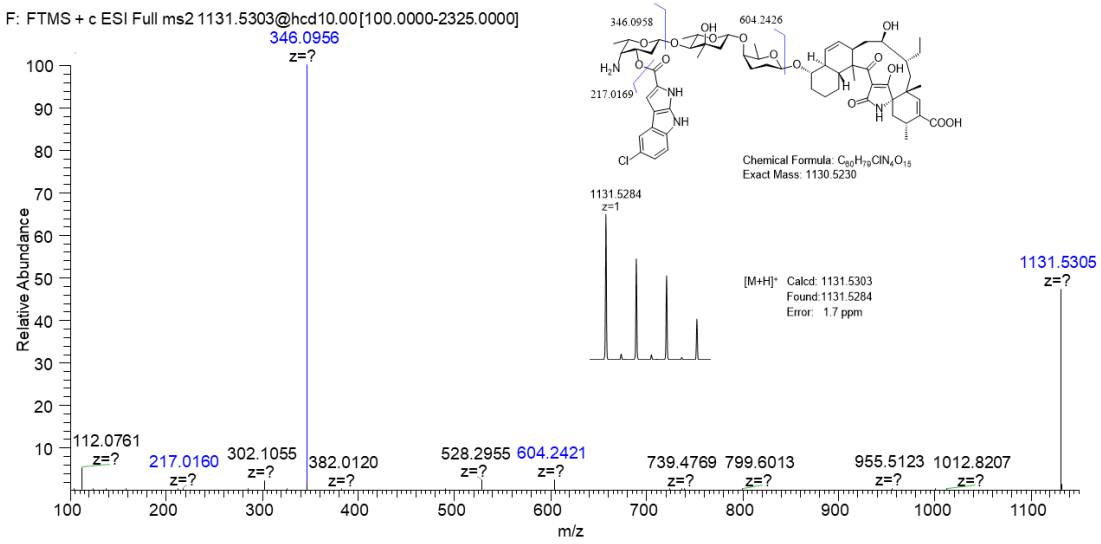

(**C**)

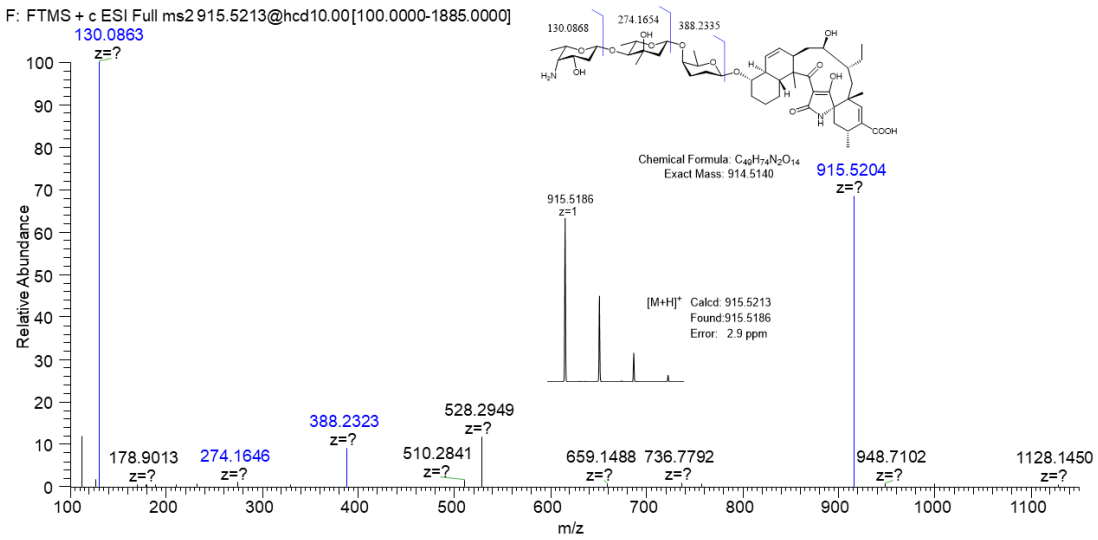
F: FTMS + c ESI Full ms2 915.5213@hcd10.00[100.0000-1885.0000]
130.0863
z=?
Relative Abundance
m/z
178.9013
z=?
274.1646
z=?
388.2323
z=?
510.2841
z=?
528.2949
z=?
659.1488
z=?
736.7792
z=?
948.7102
z=?
915.5204
z=?
1128.1450
z=?
130.0868
274.1654
388.2335
Chemical Formula: C46H74N2O14
Exact Mass: 914.5140
915.5186
z=1
[M+H]+ Calcd: 915.5213
Found:915.5186
Error: 2.9 ppm

2.2 HR-MS and HR-MS/MS analysis of 4.

Figure S4. HR-MS analysis of 4.

Qualitative Analysis Report

Data Filename	1008.d	**Sample Name**	
Sample Type	Sample	**Position**	Vial 62
Instrument Name	Instrument 1	**User Name**	
Acq Method	I3.m	**Acquired Time**	9/22/2023 2:08:36 PM
IRM Calibration Status	Success	**DA Method**	FGFUS-C18.m
Comment			

Sample Group	**Info.**
Acquisition SW Version	6200 series TOF/6500 series Q-TOF B.05.01 (B5125.3)

User Spectra

Fragmentor Voltage	Collision Energy	Ionization Mode
75	0	ESI

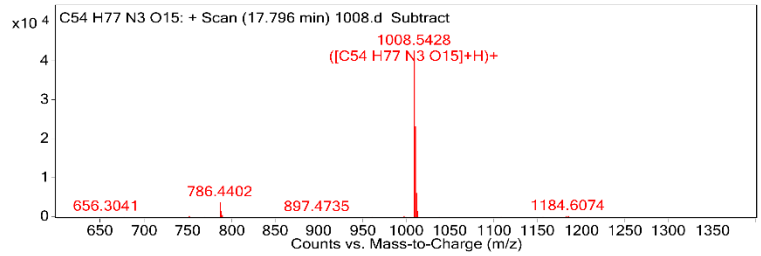

Peak List

m/z	z	Abund	Formula	Ion
1008.5428	1	40738.81	C54 H77 N3 O15	(M+H)+
1009.5456	1	23293.49	C54 H77 N3 O15	(M+H)+
1010.5460	1	6340.73	C54 H77 N3 O15	(M+H)+
1011.5474	1	1687.6	C54 H77 N3 O15	(M+H)+
1012.5512	1	310.16	C54 H77 N3 O15	(M+H)+

Formula Calculator Element Limits

Element	Min	Max
C	12	70
H	0	120
O	1	20
N	1	4

Formula Calculator Results

Ion Formula	m/z	m/z (Calc)	DBE	Diff (ppm)	Score (MFG)
C69 H72 N2 O5	1008.5428	1008.5436	35.5	0.77	99.51
C66 H74 N O8	1008.5428	1008.5409	31	-1.89	97.13
C57 H76 N4 O12	1008.5428	1008.5454	22.5	2.61	94.7
C54 H78 N3 O15	1008.5428	1008.5427	18	-0.05	100
C51 H80 N2 O18	1008.5428	1008.5401	13.5	-2.71	94.28

--- End Of Report ---

Figure S5. HR-MS/MS analysis of 4.

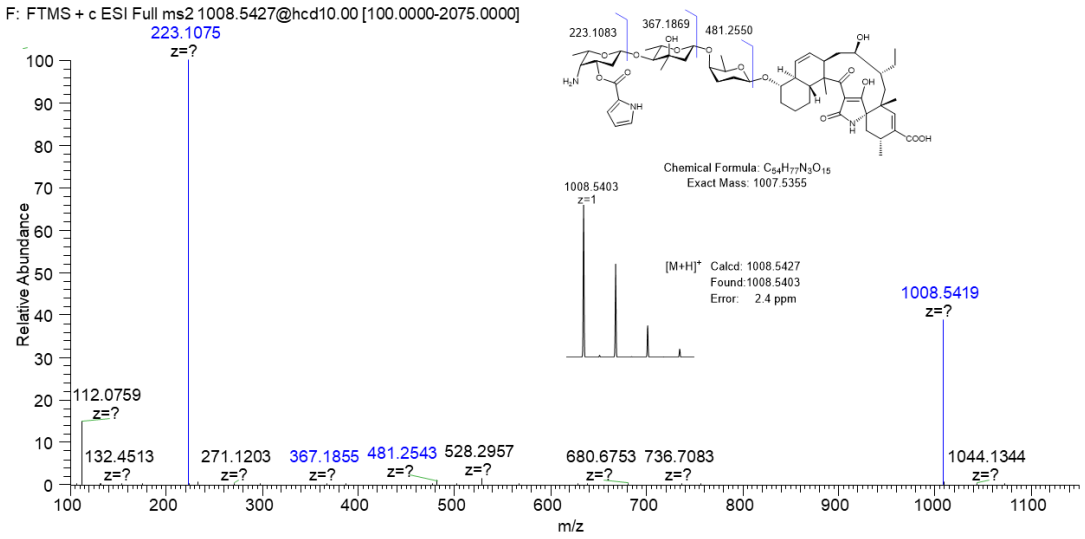

2.3 HR-MS and HR-MS/MS analysis of 5.

Figure S6. HR-MS analysis of 5.

Qualitative Analysis Report

Data Filename	1019.d	**Sample Name**	
Sample Type	Sample	**Position**	Vial 63
Instrument Name	Instrument 1	**User Name**	
Acq Method	I3.m	**Acquired Time**	9/22/2023 2:42:07 PM
IRM Calibration Status	Success	**DA Method**	FGFUS-C18.m
Comment			

Sample Group	**Info.**
Acquisition SW Version	6200 series TOF/6500 series Q-TOF B.05.01 (B5125.3)

User Spectra

Fragmentor Voltage	Collision Energy	Ionization Mode
75	0	ESI

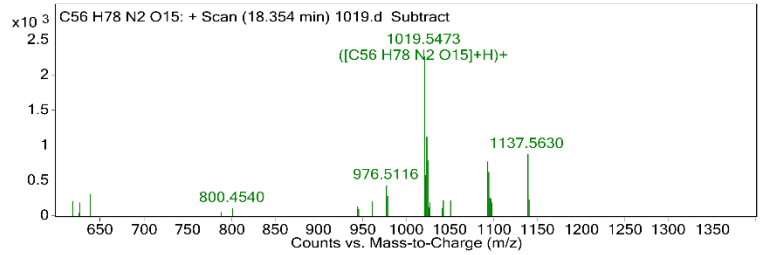

Peak List

m/z	z	Abund	Formula	Ion
1019.5473	1	2270.23	C56 H78 N2 O15	(M+H)+
1020.5464	1	1623.55	C56 H78 N2 O15	(M+H)+
1021.5513	1	600.88	C56 H78 N2 O15	(M+H)+

Formula Calculator Element Limits

Element	Min	Max
C	12	70
H	0	120
O	1	20
N	1	4

Formula Calculator Results

Ion Formula	m/z	m/z (Calc)	DBE	Diff (ppm)	Score (MFG)
C71 H73 N O5	1019.5473	1019.5483	36.5	1.01	99.16
C69 H71 N4 O4	1019.5473	1019.5470	37	-0.31	99.92
C66 H73 N3 O7	1019.5473	1019.5443	32.5	-2.94	93.31
C59 H77 N3 O12	1019.5473	1019.5502	23.5	2.82	93.8
C56 H79 N2 O15	1019.5473	1019.5475	19	0.19	99.97
C53 H81 N O18	1019.5473	1019.5448	14.5	-2.44	95.3

--- End Of Report ---

Figure S7. HR-MS/MS analysis of 5.

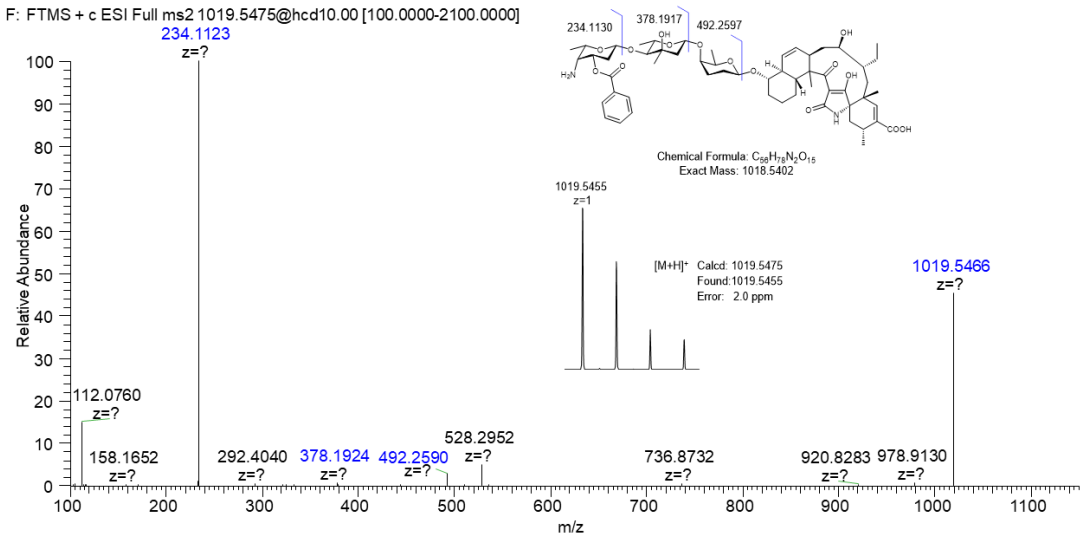

2.4 Analysis of the structure model and catalytic function of PyrK1

Figure S8. The reaction catalyzed by PrnB in pyrrolniyrin biosynthesis.[4]

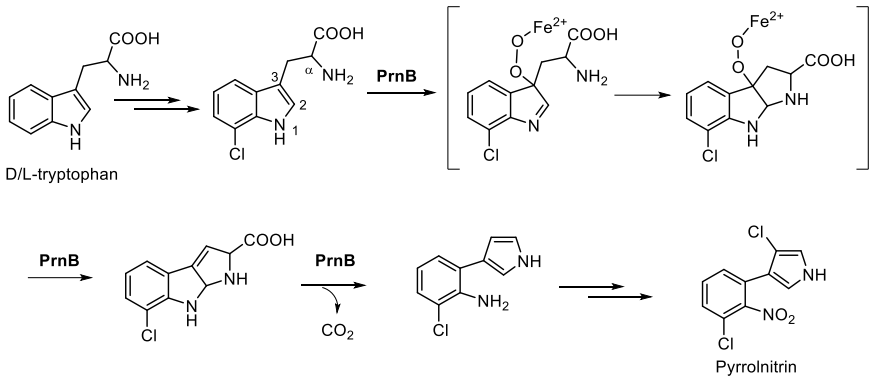

Figure S9. Structure alignment analysis of PyrK1 and PrnB. (A) Structure model of PyrK1 by AlphaFold2. **(B)** The crystal structure of PrnB (PDB:2v7j).[5] **(C)** Structure alignment of PyrK1 (blue) and PrnB (green). Both approaches give similar structures with RMSD = 1.5 Å.

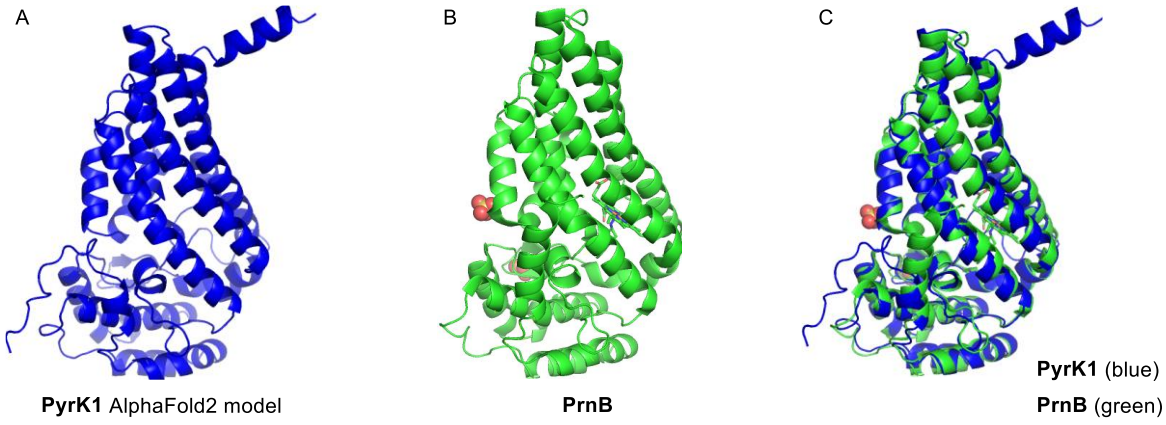

Figure S10. The known DHPI formation mechanisms. (A) Alkylation and cyclization mechamisms mediated by methyltransferases (MT),[6] prenyltransferases (PT)[7,8]. **(B)** Oxidation and cyclization mechamisms mediated cytochrome P450s[9,10,11] and flavin-dependent monooxygenases (FMO).[12,13]

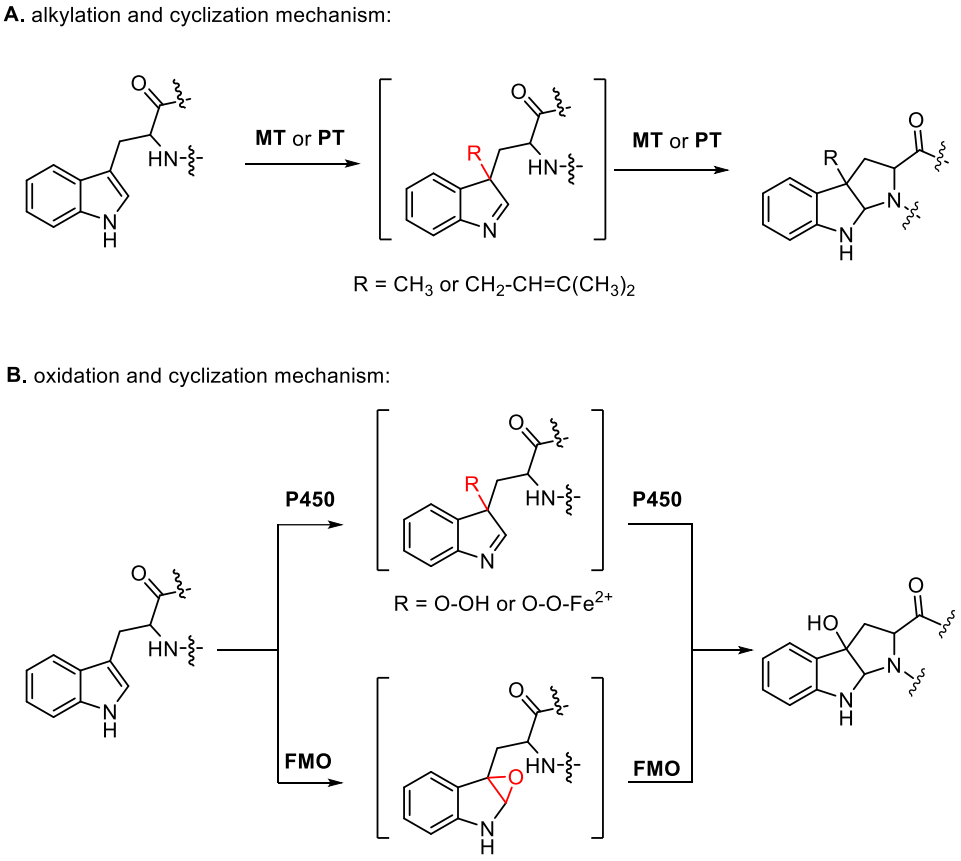

Figure S11. The proposed mechanism of PyrK1 for DHPI formation. Likely, PyrK1 initials the process by activating tryptophan through C3-peroxidative activation like PrnB,[4] followed by a nucleophilic attack of the α-amine group on the active C2 position to form the tricyclic pyrrolo[2,3-b]indole core, then, continues with peroxide elimination and oxidative desaturation to complete DHPI construction.

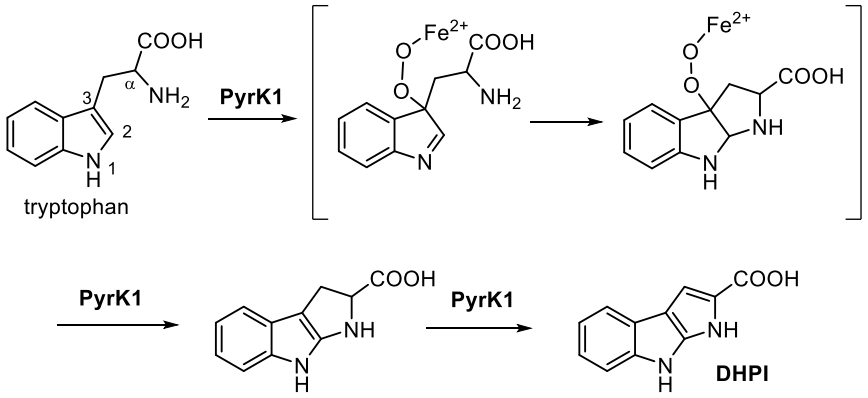

Figure S12. HPLC-MS analysis of the production of 3, 4 and 5 in *S. rugosporus*. For EICs, ESI m/z $[M + H]^+$ modes for **3**, **4**, **5**, **PYR-A** and **PYR-B** are 915.5, 1008.5, 1019.5, 1097.5 and 1131.5, respectively. (i) Wild-type strain; (ii) Δ *pyrK1* mutant strain.

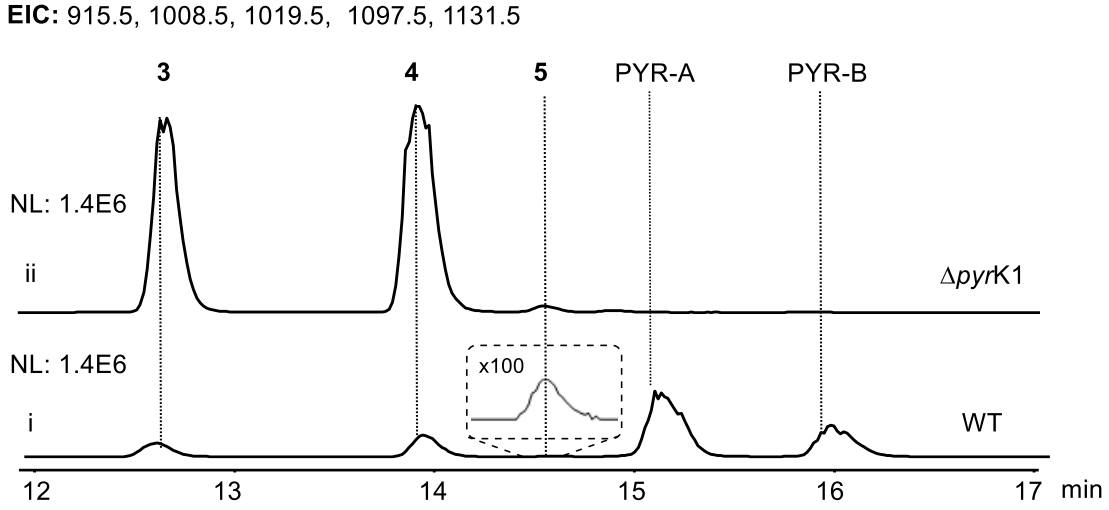

2.5 Chemical structure and NMR spectrum of 4 and 5.

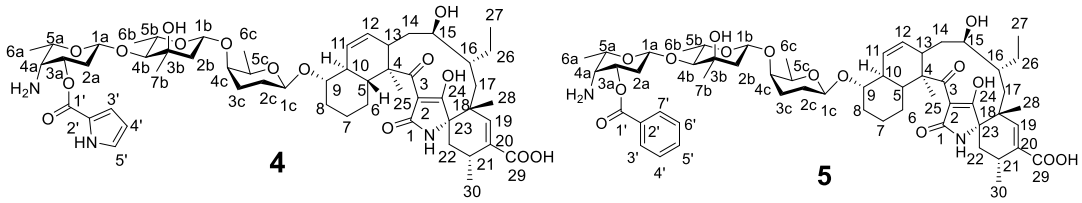

4 **5**

Table S3. ^{1}H (500 MHz) and ^{13}C NMR (125 MHz) data of 4 and 5 (δ in ppm, *J* in Hz, DMSO-d_6)

No.	4		5	
	δ_c	δ_H(*J* in Hz)	δ_c	δ_H(*J* in Hz)
1	163.0		163.8	
2	106.0		106.2	
3	201.3		200.8	
4	50.3		50.2	
5	38.8	1.33, ov	38.4	1.28, ov
6	28.5	1.12, ov	29.0	1.02, ov
		2.42, ov		2.16, t (10.2)
7	24.1	1.76, ov	24.3	1.79, ov
		1.51, ov		1.48, ov
8	35.4	1.92, ov	35.3	1.84, ov
		1.46, ov		1.73, ov
9	80.6	3.54, m	81.3	3.54, m
10	43.0	1.67, ov	44.3	1.81, ov
11	121.3	5.56, dd (14.8,7.8)	120.8	5.46, brd (14.6)
12	132.0	5.67,dd(14.8,10.8)	133.2	5.67, s
13	43.8	2.77, m	43.0	2.97, m
14	44.3	1.35, ov	44.7	1.78, ov
		1.25, ov		1.42, ov
15	81.7	3.03, ov	82.5	2.99, ov
16	43.9	0.75, m	43.2	0.78, m
17	45.3	1.82, ov	45.2	1.82, ov
		1.45, ov		1.45, ov
18	44.2		45.1	
19	146.4	6.32, s	148.0	6.29, s
20	132.0		131.7	
21	26.1	2.79, m	26.7	2.63, m
22	35.4	2.56, ov	35.3	2.54, ov
		1.42, ov		1.44, ov
23	63.1		63.1	
23NH		8.14, s		8.24, s
24	198.6		198.7	

25	14.6	1.76, s	14.6	1.49, s
26	25.1	1.43, ov	25.0	1.42, ov
		1.07, ov		1.06, ov
27	13.3	0.84, t (7.6)	13.9	0.83, t (7.6)
28	22.3	1.12, s	22.9	0.85, s
29	167.9		168.4	
30	20.8	1.17, t (7.6)	22.5	1.05, t (7.6)
1a	101.0	4.51, d (8.5)	100.8	4.51, d (9.0)
2a	34.4	2.01, ov	33.7	1.99, ov
		1.65, ov		1.71, ov
3a	66.6	3.83, m	65.7	3.84, m
4a	51.3	4.13, m	52.1	4.17, m
5a	69.7	3.58, m	69.5	3.61, m
6a	17.2	1.20, ov	17.4	1.23, ov
1b	100.1	4.73, brs	100.1	4.70, d (8.3)
2b	43.0	1.82, ov	44.5	1.83, ov
		1.44, ov		1.47, ov
3b	69.7		69.5	
4b	84.5	3.06, d (9.5)	84.3	3.05, d (8.7)
5b	68.9	3.70, m	68.9	3.64, m
6b	18.1	1.17, d (6.3)	18.5	1.16, d (7.4)
7b	27.6	1.26, s	27.6	1.19, s
1c	98.6	4.73, brs	98.5	4.69, brs
2c	24.1	1.80, ov	23.8	1.83, ov
		1.37, ov		1.38, ov
3c	24.5	1.80, ov	24.3	1.81, ov
		1.34, ov		1.32,ov
4c	75.2	3.44, m	75.2	3.46, m
5c	65.8	3.86, m	65.7	3.87, m
6c	16.9	1.11, d (6.5)	16.9	1.16, d (7.4)
1’	161.3		167.6	
2’	126.2		135.2	
3’	108.5	6.11, s	127.3	7.81, d (7.0)
4’	110.9	6.79, s	128.2	7.46, t (7.2)
5’	121.3	6.90, s	130.9	7.49, t (7.2)
6’			128.2	7.46, t (7.2)
7’			127.3	7.81, d (7.0)
4’NH		11.60, s		

In DMSO-d_6, 500 MHz for ^{1}H and 125 MHz for ^{13}C NMR. Chemical shifts were reported in ppm. ov = overlapped. All signals were determined according to COSY, HSQC, HMBC, and NOESY correlations.

Figure S13. NMR spectra of 4 in DMSO-d_6. (A) ^{1}H spectrum. **(B)** ^{13}C spectrum. **(C)** 1H-1H COSY spectrum. **(D)** HSQC spectrum. **(E)** HMBC spectrum. **(F)** NOESY spectrum.

(**A**)

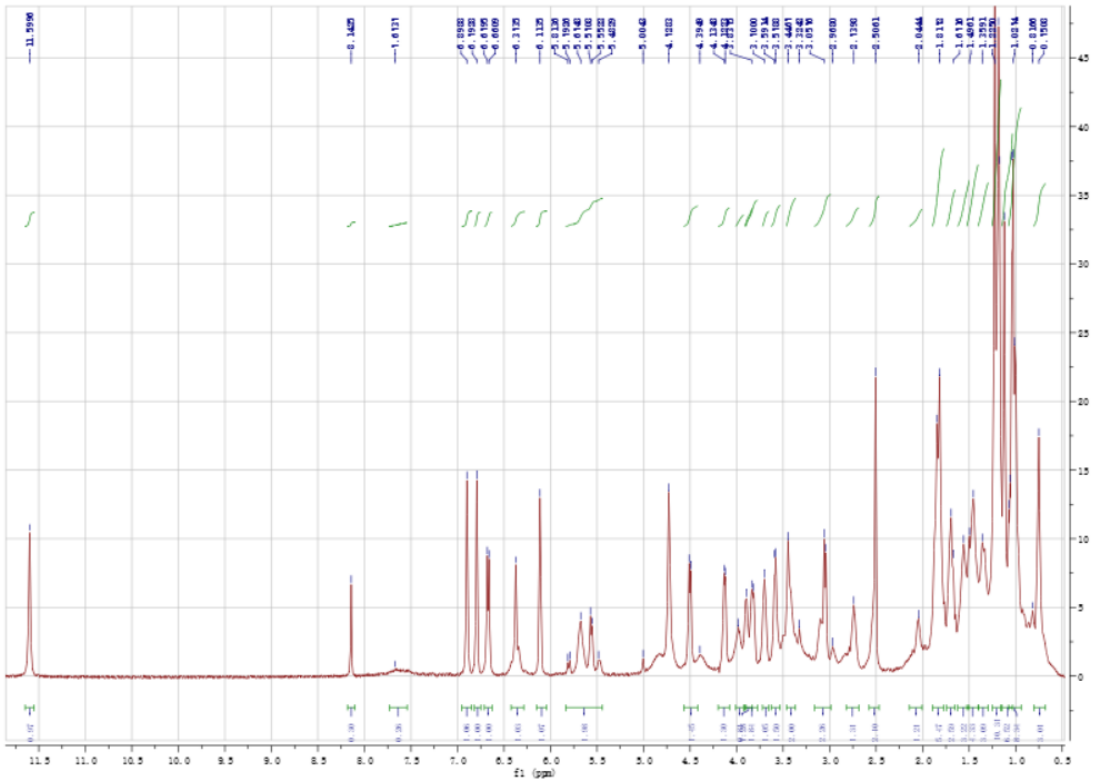

(**B**)

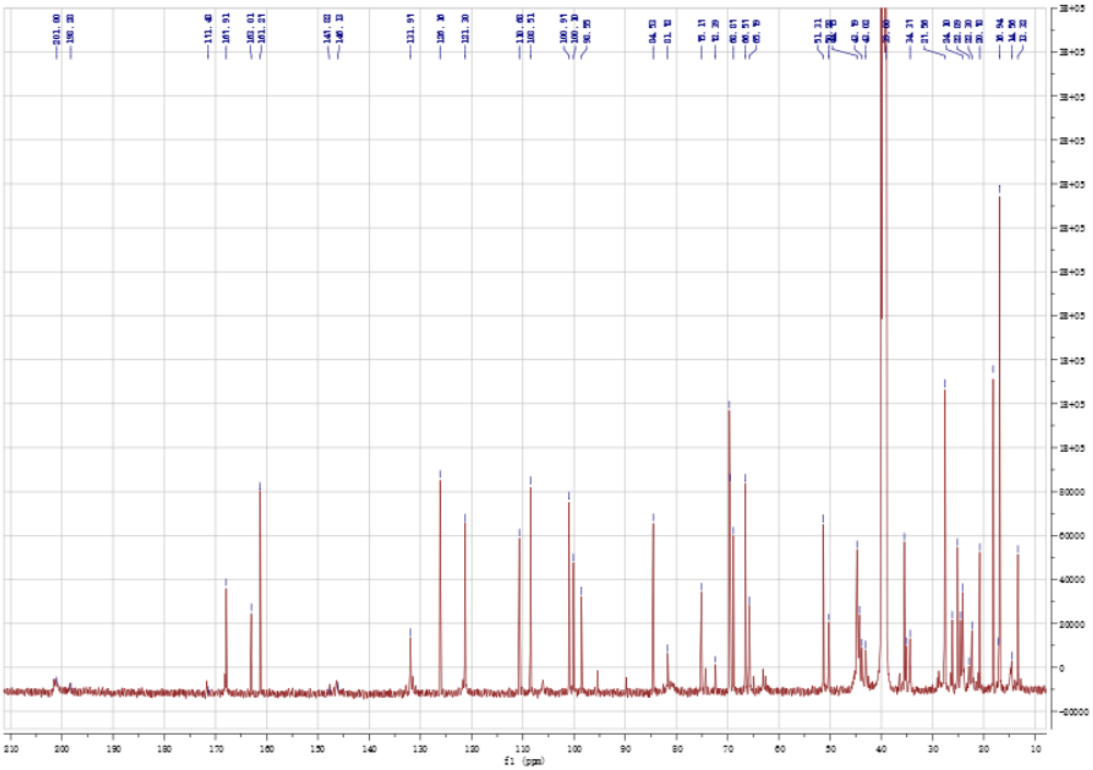

(**C**)

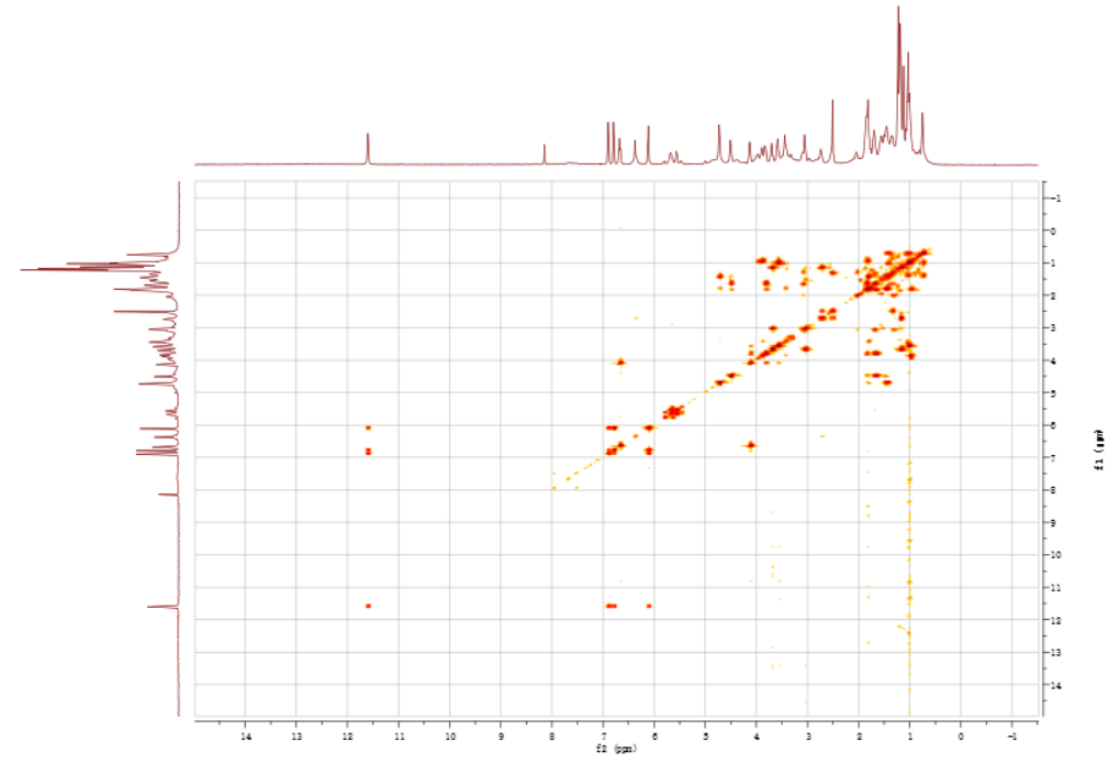

(**D**)

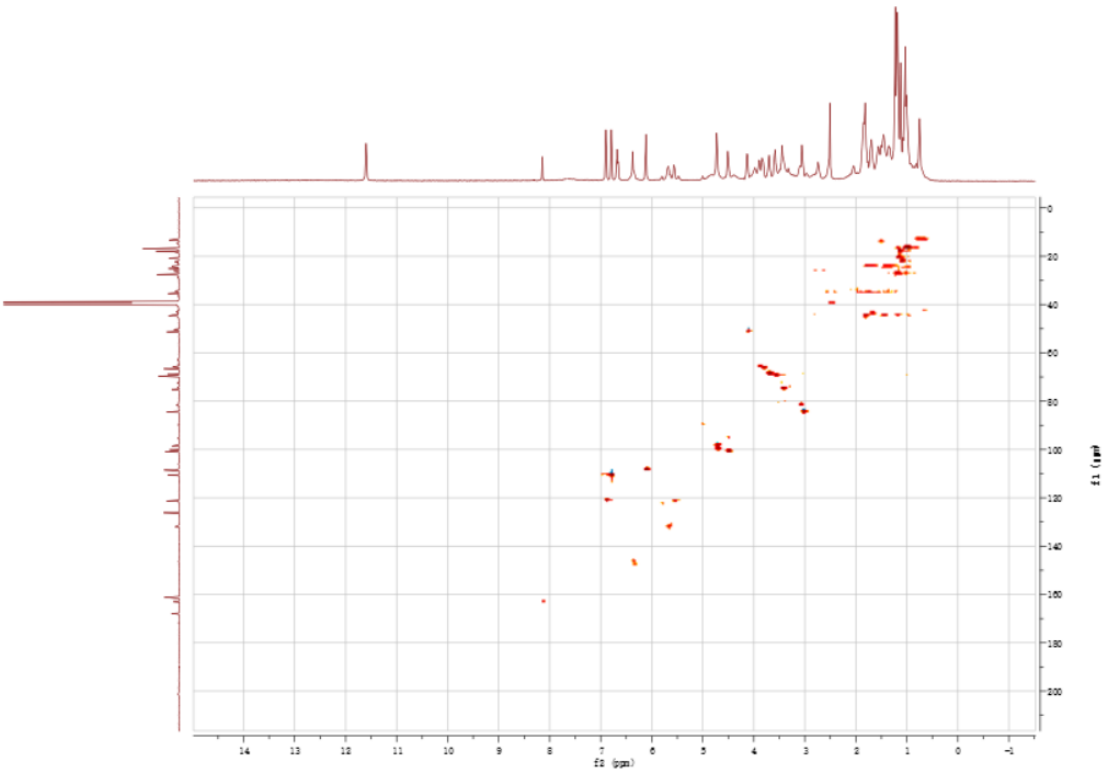

(E)

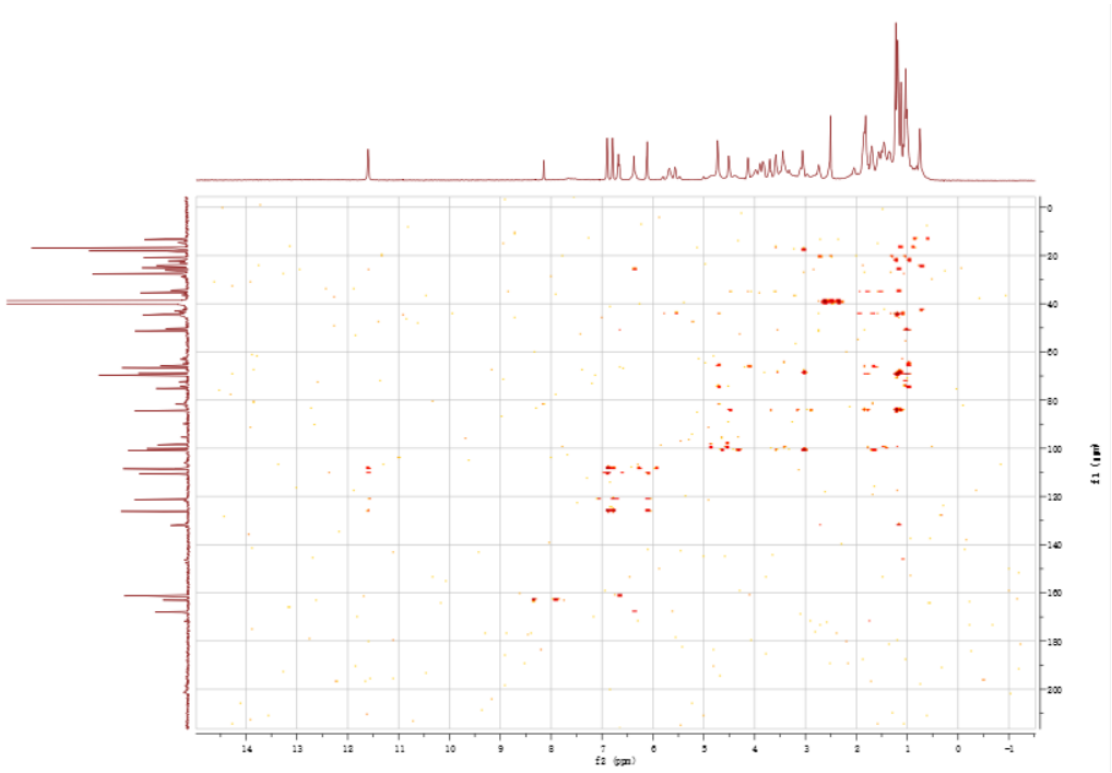

(F)

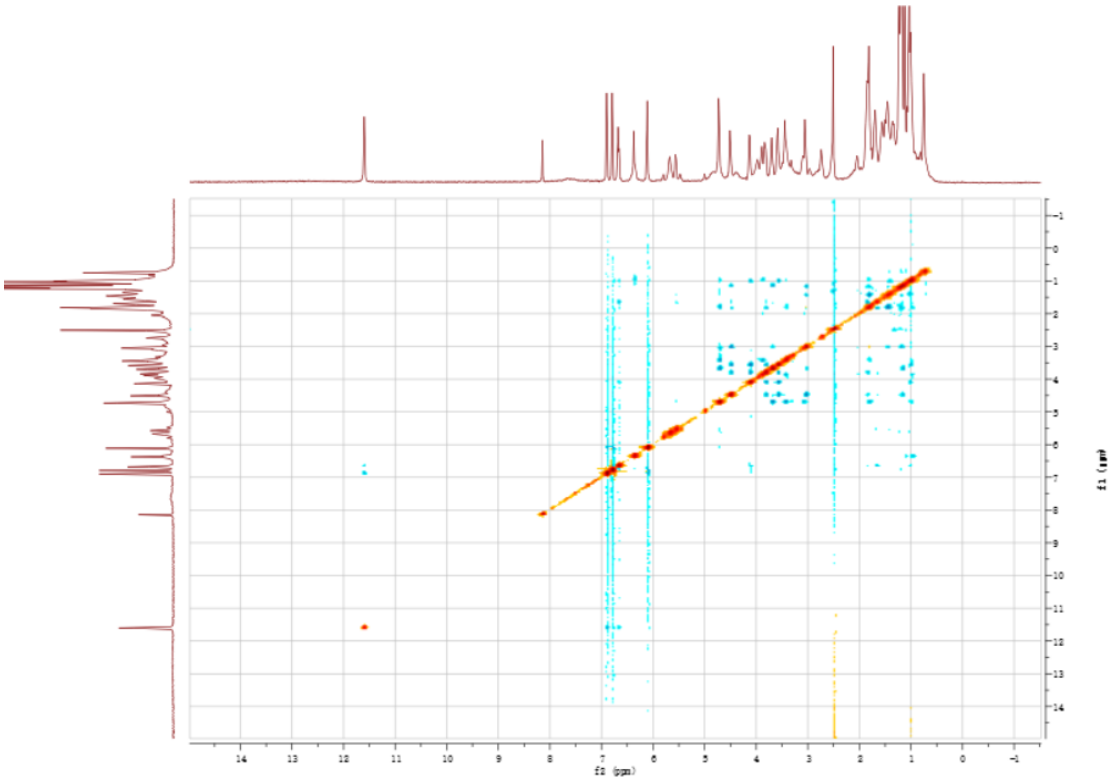

Figure S14. NMR spectra of 5 in DMSO-d_6. (A) ^{1}H spectrum. **(B)** ^{13}C spectrum. **(C)** 1H-1H COSY spectrum. **(D)** HSQC spectrum. **(E)** HMBC spectrum. **(F)** NOESY spectrum.

(**A**)

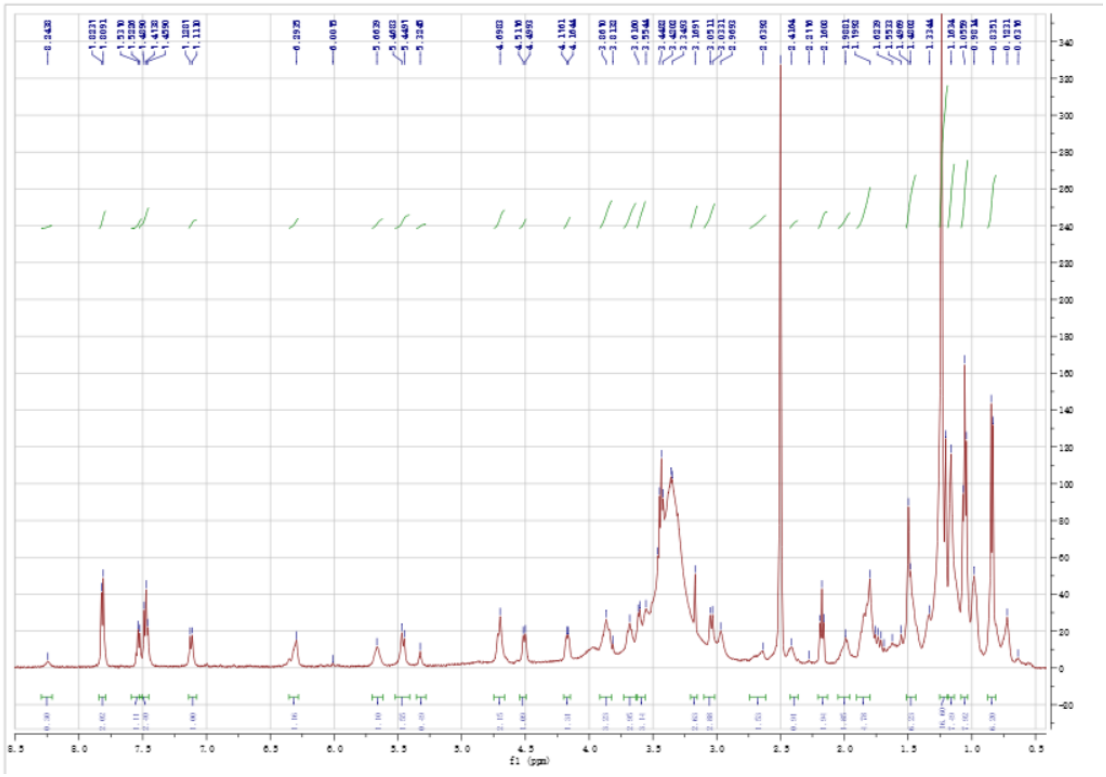

(**B**)

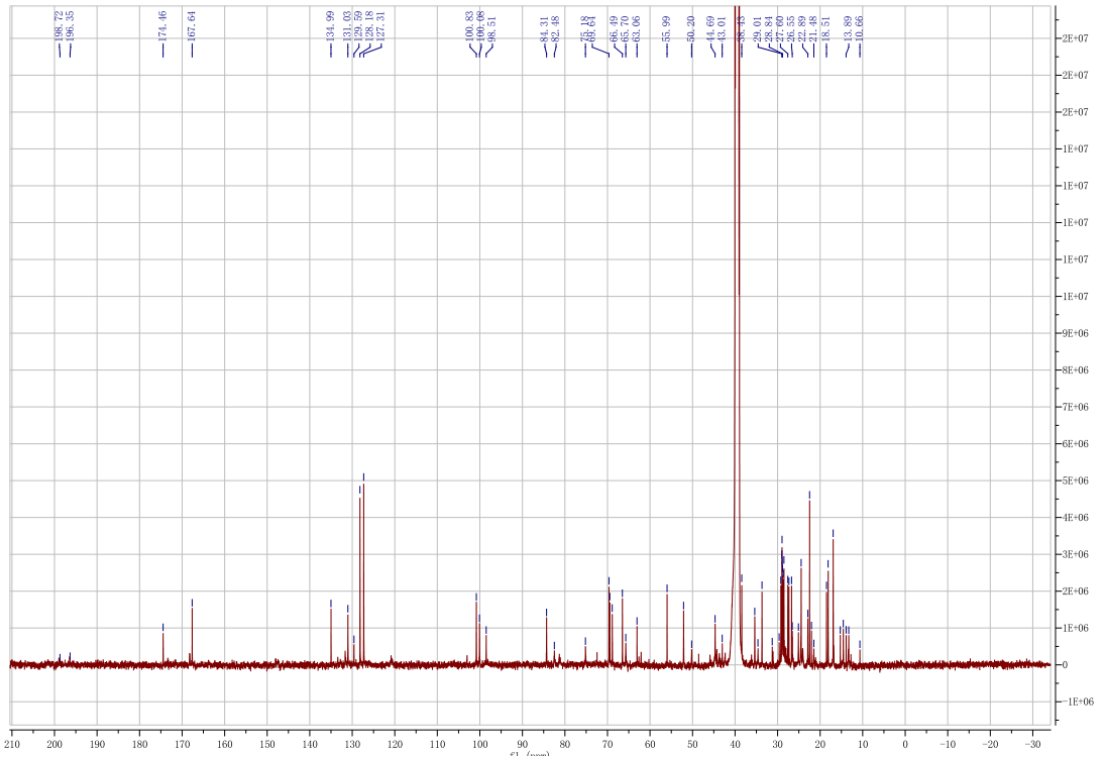

(**C**)

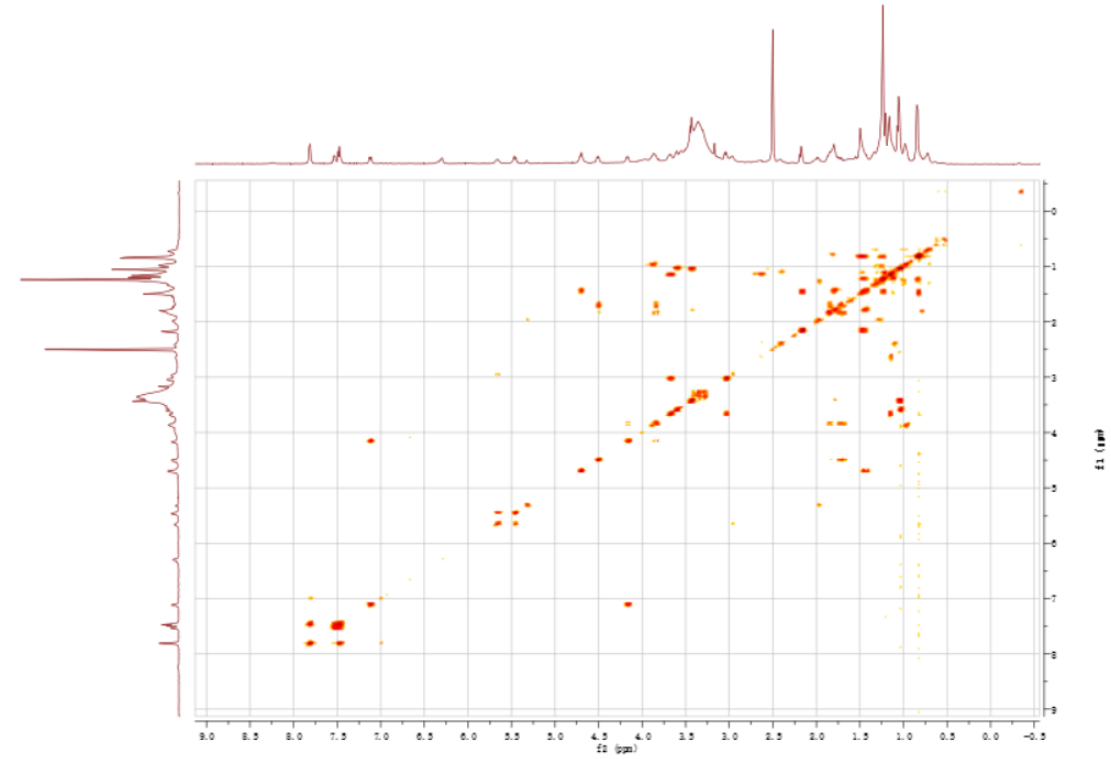

(**D**)

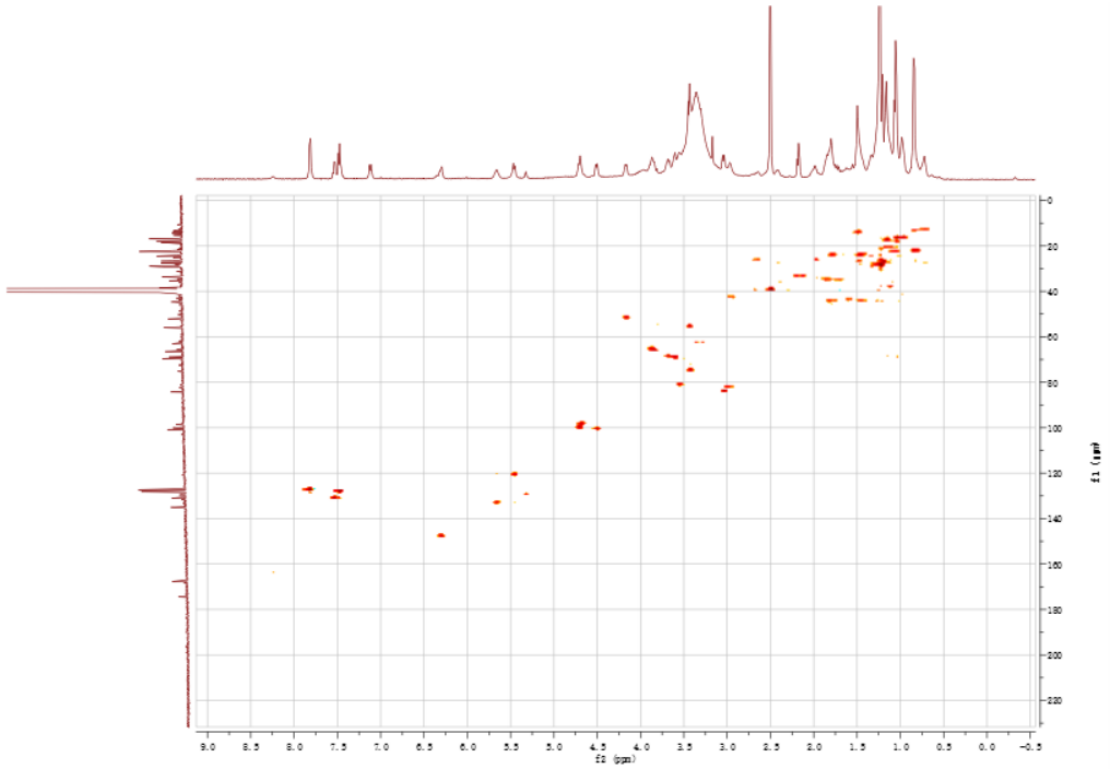

(E)

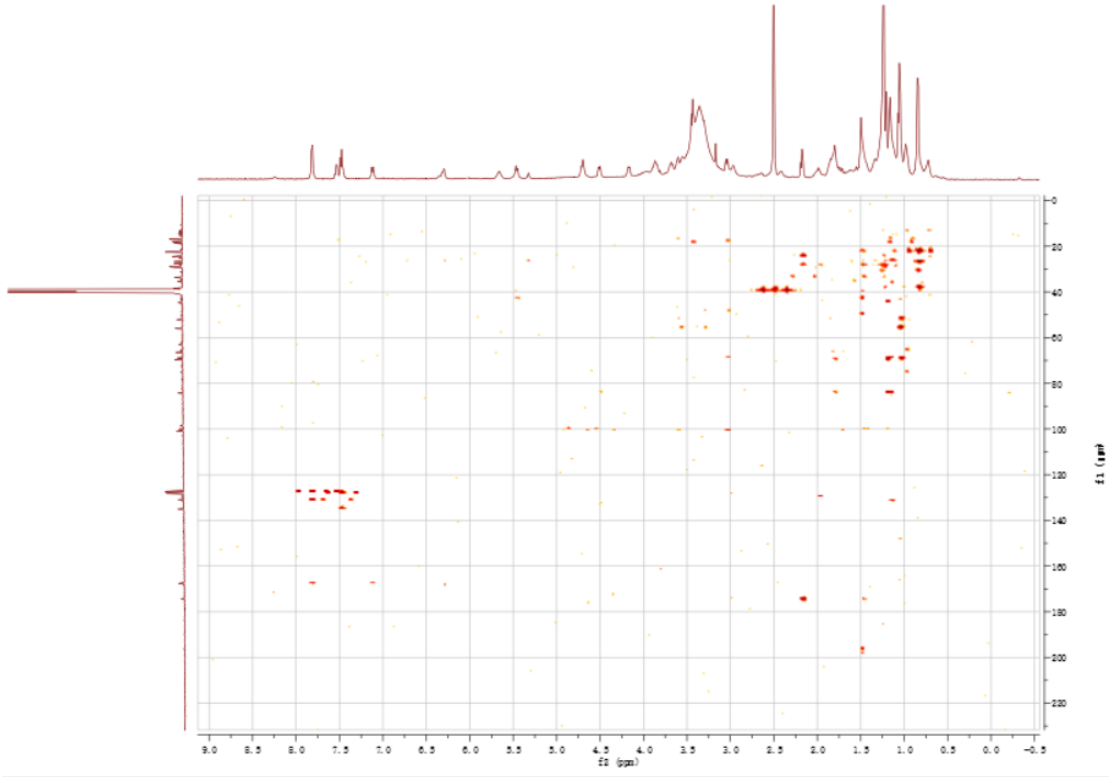

(F)

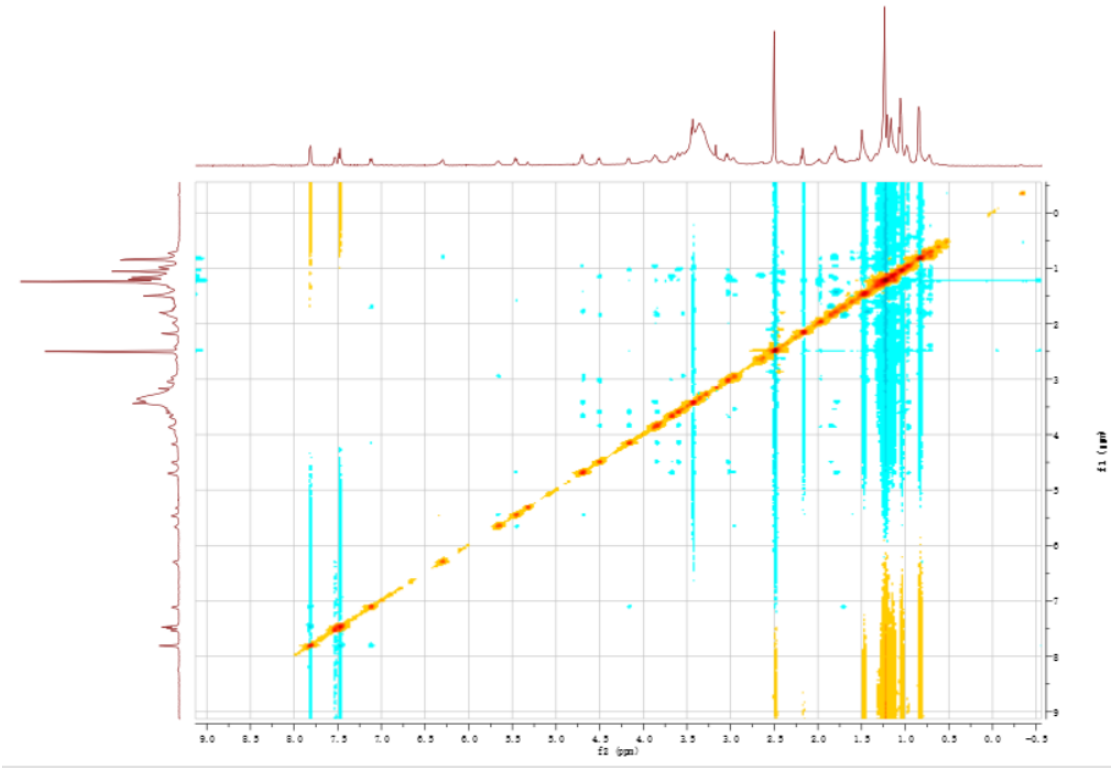

2.6 Detection of Products from Chemical Precursors Feeding.

2.6.1 Detection of product 6 from WL1001 fed with 4-aminobenzoic acid (S6).

Figure S15. HR-MS analysis of product 6

Qualitative Analysis Report

Data Filename	1034.d	**Sample Name**	3
Sample Type	Sample	**Position**	Vial 3
Instrument Name	Instrument 1	**User Name**	
Acq Method	I3.m	**Acquired Time**	9/8/2023 6:02:35 PM
IRM Calibration Status	Success	**DA Method**	Default.m
Comment			

Sample Group	**Info.**
Acquisition SW Version	6200 series TOF/6500 series Q-TOF B.05.01 (B5125.3)

User Spectra

Fragmentor Voltage	Collision Energy	Ionization Mode
75	0	ESI

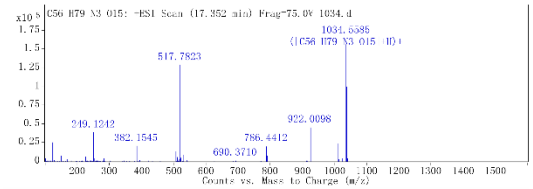

Peak List

m/z	z	Abund	Formula	Ion
1034.5585	1	157182.42	C56 H79 N3 O15	(M+H)+
1035.5613	1	100677.07	C56 H79 N3 O15	(M+H)+
1036.5617	1	25796.52	C56 H79 N3 O15	(M+H)+
1037.5642	1	5039.5	C56 H79 N3 O15	(M+H)+
1038.5631	1	949.61	C56 H79 N3 O15	(M+H)+

Formula Calculator Element Limits

Element	Min	Max
C	3	70
H	0	120
O	1	20
N	1	5

Formula Calculator Results

Ion Formula	m/z	m/z (Calc)	Diff (ppm)	DBE	Score (MFG)
C56 H80 N3 O15	1034.5585	1034.5584	-0.1	19	99.99
C69 H72 N5 O4	1034.5585	1034.5579	-0.6	37	99.7
C68 H76 N O8	1034.5585	1034.5565	-1.89	32	97.09
C61 H80 N O13	1034.5585	1034.5624	3.79	23	89.35
C51 H80 N5 O17	1034.5585	1034.5544	-3.99	15	88.34

--- End Of Report ---

Figure S16. HR-MS/MS analysis of product 6

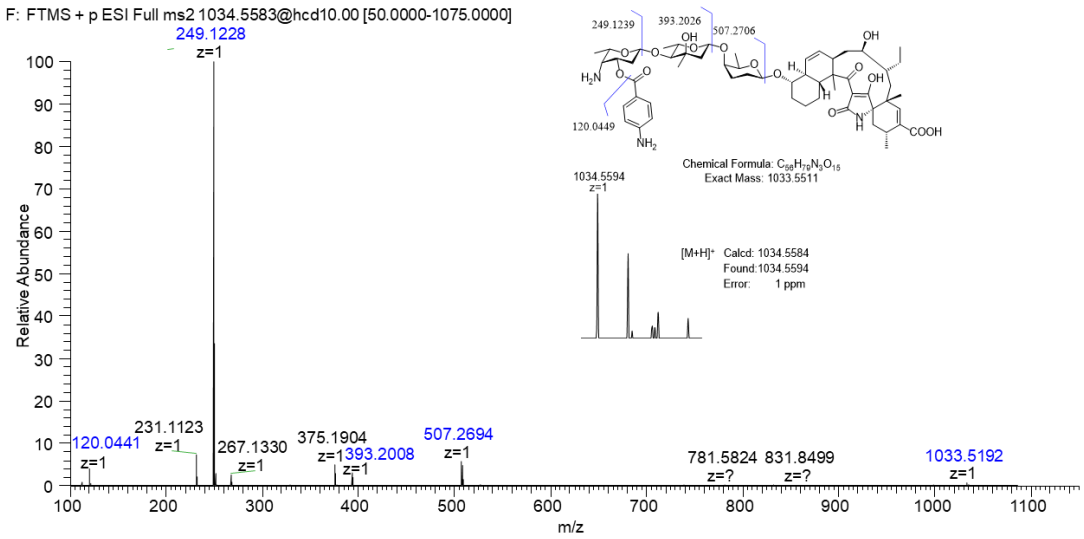

2.6.2 Detection of product 7 from WL1001 fed with 4-trifluoromethyl-benzoic acid (S7).

Figure S17. HR-MS of product 7.

Qualitative Analysis Report

Data Filename	1087.d	**Sample Name**	6
Sample Type	Sample	**Position**	Vial 6
Instrument Name	Instrument 1	**User Name**	
Acq Method	I3.m	**Acquired Time**	9/8/2023 7:43:03 PM
IRM Calibration Status	Success	**DA Method**	Default.m
Comment			

Sample Group	**Info.**
Acquisition SW Version	6200 series TOF/6500 series Q-TOF B.05.01 (B5125.3)

User Spectra

Fragmentor Voltage	Collision Energy	Ionization Mode
75	0	ESI

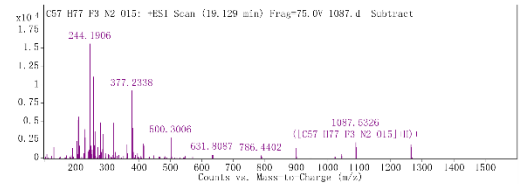

Peak List

m/z	z	Abund	Formula	Ion
1087.5326	1	2212.89	C57 H77 F3 N2 O15	(M+H)+
1088.5321	1	1615.19	C57 H77 F3 N2 O15	(M+H)+
1089.5386	1	611.02	C57 H77 F3 N2 O15	(M+H)+

Formula Calculator Element Limits

Element	Min	Max
C	3	70
H	0	120
O	1	20
N	1	5
F	1	5

Formula Calculator Results

Ion Formula	m/z	m/z (Calc)	Diff (ppm)	DBE	Score (MFG)
C63 H76 F N2 O13	1087.5326	1087.5326	0	27	100
C46 H80 F5 N4 O19	1087.5326	1087.5331	0.5	7	99.79
C49 H79 F4 N4 O18	1087.5326	1087.532	-0.55	11	99.74
C60 H77 F2 N2 O14	1087.5326	1087.5337	1.05	23	99.07
C58 H76 F5 N2 O12	1087.5326	1087.5313	-1.2	20	98.77
C52 H78 F3 N4 O17	1087.5326	1087.5309	-1.6	15	97.84
C70 H70 F3 N4 O4	1087.5326	1087.5344	1.63	37	97.78
C51 H80 F N4 O20	1087.5326	1087.5344	1.7	14	97.58
C57 H78 F3 N2 O15	1087.5326	1087.5349	2.1	19	96.36
C61 H75 F4 N2 O11	1087.5326	1087.5302	-2.25	24	95.82
C55 H77 F2 N4 O16	1087.5326	1087.5297	-2.66	19	94.31
C67 H71 F4 N4 O5	1087.5326	1087.5355	2.68	33	94.21

--- End Of Report ---

Figure S18. HR-MS/MS analysis of product 7.

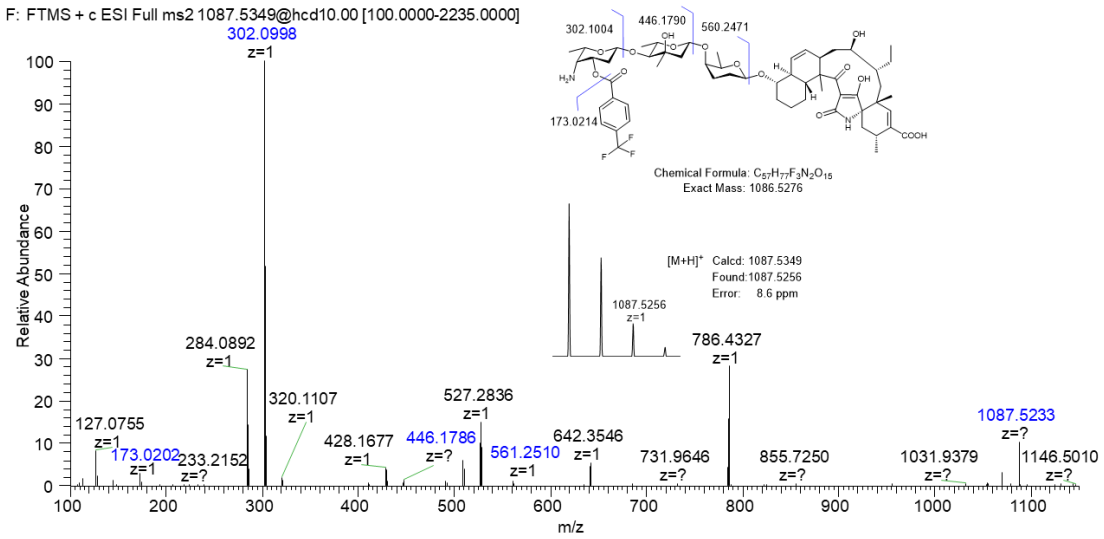

2.6.3 Detection of product 8 from WL1001 fed with 4-fluorobenzoic acid (S8).

Figure S19. HR-MS analysis of product 8.

Qualitative Analysis Report

Data Filename	1037.d	**Sample Name**	5
Sample Type	Sample	**Position**	Vial 5
Instrument Name	Instrument 1	**User Name**	
Acq Method	I3.m	**Acquired Time**	9/8/2023 7:09:31 PM
IRM Calibration Status	Success	**DA Method**	Default.m
Comment			

Sample Group	**Info.**
Acquisition SW Version	6200 series TOF/6500 series Q-TOF B.05.01 (B5125.3)

User Spectra

Fragmentor Voltage	Collision Energy	Ionization Mode
75	0	ESI

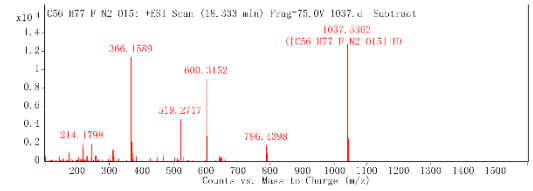

Peak List

m/z	z	Abund	Formula	Ion
1037.5362	1	12827.46	C56 H77 F N2 O15	(M+H)+
1038.5378	1	7591.61	C56 H77 F N2 O15	(M+H)+
1039.5385	1	2523.91	C56 H77 F N2 O15	(M+H)+
1040.5379	1	723.97	C56 H77 F N2 O15	(M+H)+
1041.5353	1	248.4	C56 H77 F N2 O15	(M+H)+

Formula Calculator Element Limits

Element	Min	Max
C	3	70
H	0	120
O	1	20
N	1	5
F	1	5

Formula Calculator Results

Ion Formula	m/z	m/z (Calc)	Diff (ppm)	DBE	Score (MFG)
C64 H70 F5 N4 O3	1037.5362	1037.5363	0.06	30	100
C45 H80 F3 N4 O19	1037.5362	1037.5363	0.13	7	99.99
C54 H77 F4 N2 O13	1037.5362	1037.5356	-0.55	16	99.75
C51 H78 F5 N2 O14	1037.5362	1037.5368	0.55	12	99.74
C48 H79 F2 N4 O18	1037.5362	1037.5352	-0.97	11	99.22
C67 H69 F4 N4 O2	1037.5362	1037.5351	-1.05	34	99.09
C42 H81 F4 N4 O20	1037.5362	1037.5375	1.24	3	98.74
C69 H70 F N4 O4	1037.5362	1037.5376	1.31	37	98.57
C57 H76 F3 N2 O12	1037.5362	1037.5345	-1.65	20	97.76
C56 H78 F N2 O15	1037.5362	1037.5381	1.81	19	97.33
C51 H78 F N4 O17	1037.5362	1037.5341	-2.07	15	96.53
C70 H68 F3 N4 O	1037.5362	1037.534	-2.15	38	96.28
C66 H71 F2 N4 O5	1037.5362	1037.5387	2.42	33	95.34
C60 H75 F2 N2 O11	1037.5362	1037.5333	-2.76	24	94.03
C53 H79 F2 N2 O16	1037.5362	1037.5392	2.91	15	93.39

--- End Of Report ---

Figure S20. HR-MS/MS analysis of product 8.

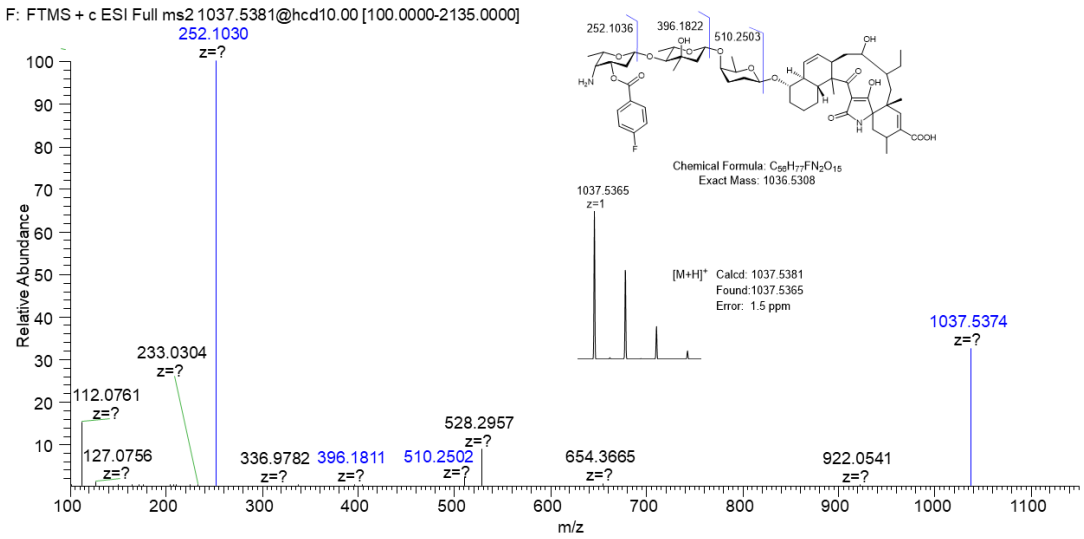

2.6.4 Detection of product 9 from WL1001 fed with thiophene-2-carboxylic acid (S9).

Figure S21. HR-MS analysis of product 9.

Qualitative Analysis Report

Data Filename	1025.d	**Sample Name**	Sample35
Sample Type	Sample	**Position**	Vial 24
Instrument Name	Instrument 1	**User Name**	
Acq Method	I3.m	**Acquired Time**	1/29/2024 2:14:59 PM
IRM Calibration Status	Success	**DA Method**	Default.m
Comment			

Sample Group	**Info.**
Acquisition SW Version	6200 series TOF/6500 series Q-TOF B.05.01 (B5125.3)

User Spectra

Fragmentor Voltage	Collision Energy	Ionization Mode
75	0	ESI

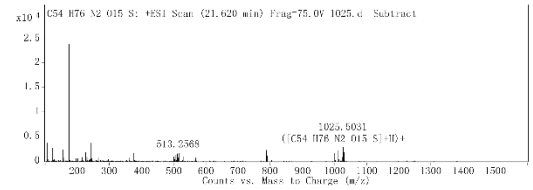

Peak List

m/z	z	Abund	Formula	Ion
1025.5031	1	2991.11	C54 H76 N2 O15 S	(M+H)+
1026.5041	1	1966.57	C54 H76 N2 O15 S	(M+H)+
1027.5013	1	1011.16	C54 H76 N2 O15 S	(M+H)+
1028.5030	1	308.06	C54 H76 N2 O15 S	(M+H)+

Formula Calculator Element Limits

Element	Min	Max
C	3	70
H	0	120
O	1	20
N	1	5
S	1	2

Formula Calculator Results

Ion Formula	m/z	m/z (Calc)	Diff (ppm)	DBE	Score (MFG)
C46 H81 N4 O17 S2	1025.5031	1025.5033	0.16	9	99.98
C67 H69 N4 O4 S	1025.5031	1025.5034	0.3	36	99.93
C54 H77 N2 O15 S	1025.5031	1025.5039	0.8	18	99.47
C58 H77 N2 O10 S2	1025.5031	1025.5014	-1.65	22	97.79
C49 H77 N4 O17 S	1025.5031	1025.4999	-3.13	14	92.49
C64 H73 N4 O4 S2	1025.5031	1025.5068	3.59	31	90.38

--- End Of Report ---

Figure S22. HR-MS/MS analysis of product 9.

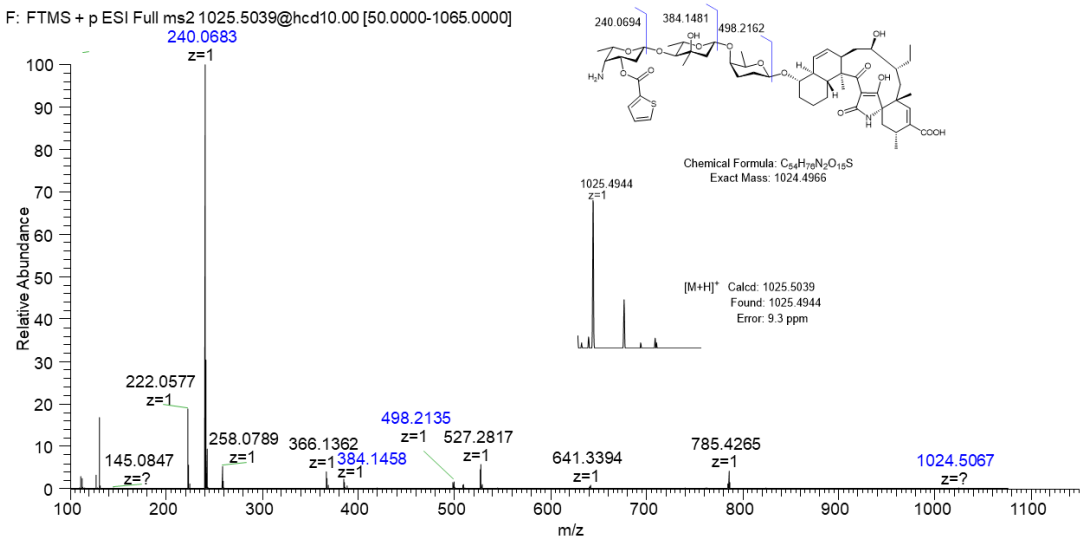

2.6.5 Detection of product 10 from WL1001 fed with 1H-indole-2-carboxylic acid (S10).

Figure S23. HR-MS analysis of product 10.

Qualitative Analysis Report

Data Filename	yinduo2-1.d	**Sample Name**	Sample35
Sample Type	Sample	**Position**	Vial 25
Instrument Name	Instrument 1	**User Name**	
Acq Method	I3.m	**Acquired Time**	1/29/2024 2:48:25 PM
IRM Calibration Status	Success	**DA Method**	Default.m
Comment			

Sample Group	**Info.**
Acquisition SW Version	6200 series TOF/6500 series Q-TOF B.05.01 (B5125.3)

User Spectra

Fragmentor Voltage	Collision Energy	Ionization Mode
75	0	ESI

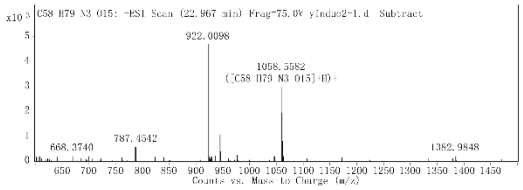

Peak List

m/z	z	Abund	Formula	Ion
1058.5582	1	3003.54	C58 H79 N3 O15	(M+H)+
1059.5562	1	1963.25	C58 H79 N3 O15	(M+H)+
1060.564	1	845	C58 H79 N3 O15	(M+H)+
1061.5719	1	234	C58 H79 N3 O15	(M+H)+
1382.9848		238.64		

Formula Calculator Element Limits

Element	Min	Max
C	3	60
H	0	120
O	1	30
N	1	5

Formula Calculator Results

Ion Formula	m/z	m/z (Calc)	Diff (ppm)	DBE	Score (MFG)
C58 H80 N3 O15	1058.5582	1058.5584	0.18	21	99.97
C45 H88 N O26	1058.5582	1058.5589	0.67	3	99.62
C70 H76 N O8	1058.5582	1058.5565	-1.57	34	97.97
C46 H84 N5 O22	1058.5582	1058.5602	1.93	8	96.93
C53 H80 N5 O17	1058.5582	1058.5544	-3.62	17	90.09
C63 H80 N O13	1058.5582	1058.5624	3.99	25	88.25
C52 H84 N O21	1058.5582	1058.5530	-4.88	12	83.51

--- End Of Report ---

Figure S24. HR-MS/MS analysis of product 10.

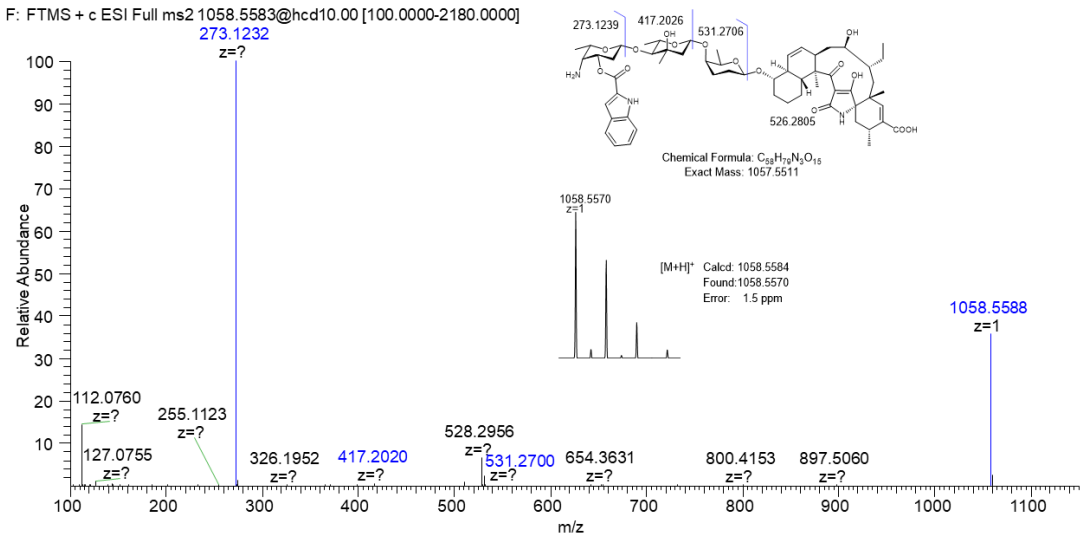

2.6.6 Detection of product 11 from WL1001 fed with 1H-indole-5-carboxylic acid (S11).

Figure S25. HR-MS analysis of product 11.

Qualitative Analysis Report

Data Filename	1058-5.d	**Sample Name**	4
Sample Type	Sample	**Position**	Vial 4
Instrument Name	Instrument 1	**User Name**	
Acq Method	I3.m	**Acquired Time**	9/8/2023 6:36:05 PM
IRM Calibration Status	Success	**DA Method**	Default.m
Comment			

Sample Group	**Info.**
Acquisition SW Version	6200 series TOF/6500 series Q-TOF B.05.01 (B5125.3)

User Spectra

Fragmentor Voltage	Collision Energy	Ionization Mode
75	0	ESI

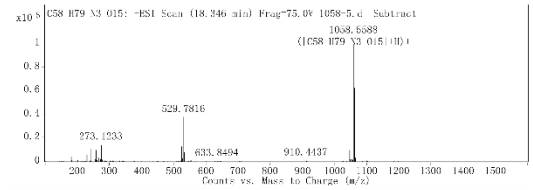

Peak List

m/z	z	Abund	Formula	Ion
1058.5588	1	99702.39	C58 H79 N3 O15	(M+H)+
1059.5613	1	62705.68	C58 H79 N3 O15	(M+H)+
1060.5639	1	17392.91	C58 H79 N3 O15	(M+H)+
1061.5655	1	3838.68	C58 H79 N3 O15	(M+H)+
1062.5655	1	899.1	C58 H79 N3 O15	(M+H)+

Formula Calculator Element Limits

Element	Min	Max
C	3	70
H	0	120
O	1	20
N	1	5

Formula Calculator Results

Ion Formula	m/z	m/z (Calc)	Diff (ppm)	DBE	Score (MFG)
C58 H80 N3 O15	1058.5588	1058.5584	-0.38	21	99.88
C70 H76 N O8	1058.5588	1058.5565	-2.13	34	96.29

--- End Of Report ---

Figure S26. HR-MS/MS analysis of product 11.

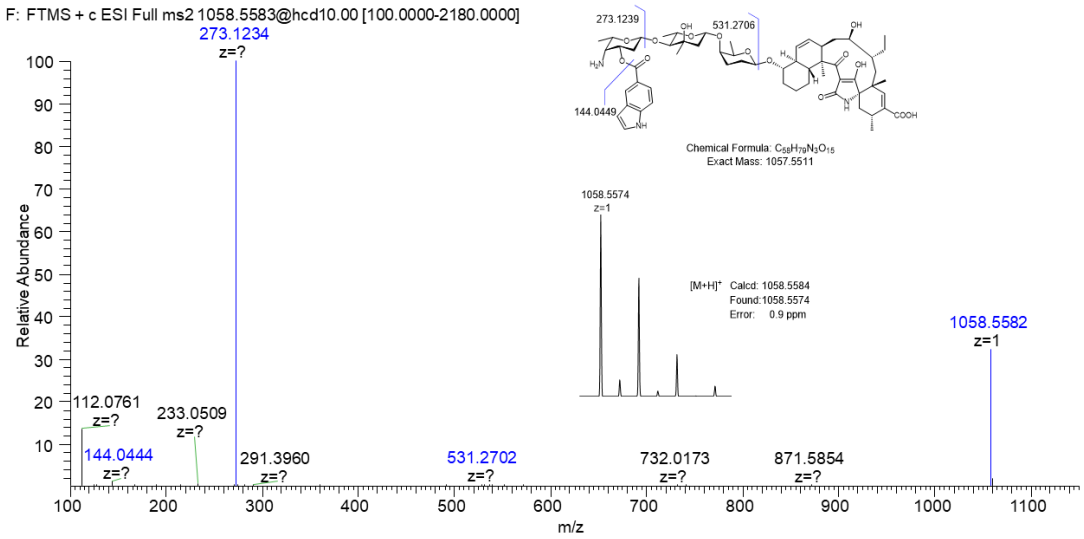

3 Supplementary references

1. M.R. Green, J.Sambrook, Molecular Cloning: A Laboratory Manual 4 th edn, 2012.
2. T.Keiser, M.J. Bibb, M.J.Buttner, K.F.Chater, D.A.Hopwood, Practical Streptomyces Genetics, 2000.
3. Q. Wu, Z. Wu, X. Qu and W. Liu, Insights into pyrroindomycin biosynthesis reveal a uniform paradigm for tetramate/tetronate formation, *J. Am. Chem. Soc.*, 2012, **134**, 17342-17345.
4. W. De Laurentis, L. Khim, J. L. Anderson, A. Adam, K. A. Johnson, R. S. Phillips, S. K. Chapman, K. H. van Pee and J. H. Naismith, The second enzyme in pyrrolnitrin biosynthetic pathway is related to the heme-dependent dioxygenase superfamily, *Biochemistry*, 2007, **46**, 12393-12404.
5. X. Zhu, K. H. van Pee and J. H. Naismith, The ternary complex of PrnB (the second enzyme in the pyrrolnitrin biosynthesis pathway), tryptophan, and cyanide yields new mechanistic Insights into the indolamine dioxygenase superfamily, *J. Biol. Chem.*, 2010, **285**, 21126-21133.
6. J. Liu, T. Ng, Z. Rui, O. Ad and W. Zhang, Unusual Acetylation-Dependent Reaction Cascade in the Biosynthesis of the Pyrroloindole Drug Physostigmine, *Angew. Chem. Int. Ed.*, 2014, **126**, 140-143.
7. J. M. Schuller, G. Zocher, M. Liebhold, X. Xie, M. Stahl, S. M. Li and T. Stehle, Structure and catalytic mechanism of a cyclic dipeptide prenyltransferase with broadsubstrate promiscuity, *J. Mol. Biol.*, 2012, **422**, 87–99.
8. E. T. Miller, O. V. Tsodikov and S. Garneau-Tsodikova, Structural insights into the diverse prenylating capabilities of DMATS prenyltransferases, *Nat. Prod. Rep.*, 2024, **41**, 113–147.
9. W. Y. Tian, C. H. Sun, M. Zheng, J. R. Harmer, M. J. Yu, Y. A. Zhang, H. D. Peng, D. Q. Zhu, Z. X. Deng, S. L. Chen, M. Mobli, X. Y. Jia, X. D. Qu, Efficient biosynthesis of heterodimeric C3-aryl pyrroloindoline alkaloids, *Nat. Commun.*, 2018, **9**, 4428-4436.
10. T. Saruwatari, F. Yagishita, T. Mino, H. Noguchi, K. Hotta, K. Watanabe, Cytochrome P450 as Dimerization Catalyst in Diketopiperazine Alkaloid Biosynthesis, *ChemBioChem*, 2014, **15**, 656-659.
11. B. D. Ames, X. Y. Liu, C.T. Walsh, Enzymatic Processing of Fumiquinazoline F: A Tandem Oxidative-Acylation Strategy for the Generation of Multicyclic Scaffolds in Fungal Indole Alkaloid Biosynthesis, *Biochemistry*, 2010, **49**, 8564-8576.
12. S. Y. Li, J. M. Finefield, J. D. Sunderhaus, T. J. McAfoos, R. M. Williams, D. H. Sherman, Biochemical Characterization of NotB as an FAD-Dependent Oxidase in the Biosynthesis of Notoamide Indole Alkaloids, *J. Am. Chem. Soc.*, 2012, **134**, 788-791.
13. C. Sun, W. Tian, Z. Lin and X. Qu, Biosynthesis of pyrroloindoline-containing natural products, *Nat. Prod. Rep.*, 2022, **39**, 1721-1765.